THE VARIATION OF THE ANOMALOUS POSITRON LIFETIME WITH TEMPERATURE IN SOLIDS

By

GERALD DEAN LOPER, JR.

Bachelor of Arts

University of Wichita

Wichita, Kansas

1959

Submitted to the faculty of the Graduate School of
the Oklahoma State University
in partial fulfillment of the requirements
for the degree of
MASTER OF SCIENCE
May, 1962

THE VARIATION OF THE ANOMALOUS POSITRON LIFETIME
WITH TEMPERATURE IN SOLIDS

Thesis Approved:

B. Clark Grosecloss
Thesis Adviser

K. C. Harrington

Dean of the Graduate School

PREFACE

In molecular materials, positrons exhibit two distinct lifetimes. One, of the order of 10^{-10} second, is due to free annihilation and annihilation from the singlet state of the bound system positronium. The other, of the order of 10^{-9} second, is due to the annihilation of the positron from the triplet state of positronium with a lattice electron of opposite spin. This longer lifetime is sometimes referred to as the anomalous positron lifetime.

The variation of the anomalous positron lifetime with temperature has been studied in only a few solids. In this experiment, the study of this variation was extended to three polymers and the data were related to specific volume or density changes caused by changes in temperature. Increasing the temperature of a solid increases its free volume. The positronium atoms seek out the free volume, where there is smaller probability of annihilation with a lattice electron. Thus the lifetime is lengthened.

The author would like to express his gratitude to his major adviser, Dr. B.C. Groseclose for his help and encouragement throughout the experiment. Use of the equipment was shared with Mr. J.L. Pigg and Mr. R.D. Eagleton, both of whom were helpful and patient during data taking times. Dr. E.E. Kohnke and Dr. K.D. Berlin gave valuable suggestions concerning the properties of samples used in the experiment, and Mr. Heinz Hall, Mr. Frank Hargrove, and Mr. Richard Gruhlkey

of the Physics Shop were most helpful in preparing the samples. The author also extends his appreciation to his wife, Joyce Loper, who was not only patient and understanding during the experiment, but also typed this thesis.

TABLE OF CONTENTS

LIST OF TABLES

LIST OF FIGURES

CHAPTER I

INTRODUCTION: THEORY AND PREVIOUS RESULTS

Dirac's Theory

Dirac's relativistic quantum-mechanical theory of the electron predicted a continuum of negative energy states as well as a continuum of positive states. This was at first thought to have no physical significance, but the identification of the positron by Anderson (1) in cloud chamber photographs of cosmic-ray particles brought about the explanation of electron phenomena through this idea of negative energy levels.

The assumptions of this theory are that all the negative energy states (they range from $-mc^2$ to $-\infty$ for free electrons) are filled up with electrons; these electrons do not produce an external field and do not contribute to the total charge, energy, and momentum of the system. A filled positive level is interpreted as a moving electron, while an empty negative level is a moving positron. Annihilation of a pair requires the transition of the electron into the hole representing the positron. In this process charge is conserved, but the total number of particles is not. The energy created ($\geq 2mc^2$) is given off as radiation.

Positronium Formation and Annihilation

The experiments of de Benedetti, et. al. (2) have shown that most positrons in solids slow down to very low energies before annihilating. Mohorovičić (3) proposed that a bound state like the hydrogen atom could be formed by an electron and positron after the positron slowed down, and Ruark (4) suggested the name positronium for the system. The existence of such a state was later verified experimentally by Deutsch (5,6). Wheeler (7) noted that the energy levels of positronium are obtained easily by comparison with the values for an idealized hydrogen atom with an infinitely great nuclear mass. The potential energy in both cases is of the same form, $-e^2/r$ where r is the distance between charges, and the kinetic energy of the positronium system is only half that of the hydrogen atom due to the reduced mass. The expression for the energy of the n^{th} quantum state of positronium is then

$$E_n = -\frac{\pi^2 m e^4}{n^2 h^2} \quad . \tag{1}$$

The wave function for the ground state of positronium is

$$\psi = \pi^{-\frac{1}{2}} \left(\frac{1}{2a_0}\right)^{3/2} \exp\left(-\frac{r}{2a_0}\right) \tag{2}$$

where

$$a_0 = \frac{h^2}{me^2} \tag{3}$$

is the Bohr radius for the hydrogen atom.

The energetics of positronium formation can be visualized by use of the "Ore gap" idea. Let the positronium binding energy be E_p and the ionization potential of an atom of a

material be E_i. The range of energies over which positronium formation can take place, called the "Ore gap", is limited by these factors and E_e, the lowest excitation potential of the surrounding atoms. See Figure 1 for a diagram of the Ore gap.

Positronium formation is possible if the initial energy of a positron is greater than the difference $E_i - E_p$. Above E_e, inelastic scattering of the positron is a competing process and makes positronium formation unlikely. Below the value of $E_i - E_p$ the positron does not have enough energy to capture an electron. The ratio of the width of the Ore gap to the width from zero to E_e gives the fraction of the positrons which will form positronium providing it is assumed that the positrons are evenly distributed in energy between zero and E_e (8,9,10).

Annihilation of a positron and electron can occur with either one as a free particle, or from the bound state of positronium, which is unstable. The discussion of annihilation will be limited to low relative kinetic energies for the particles; that is, only S states are of interest. In the singlet ^1S state, the spins of the particles are anti-parallel and the total angular momentum is zero. Two gamma rays are emitted upon annihilation from this state. The spins of particles in the triplet ^3S state are parallel so that the total angular momentum is one. This state annihilates with the emission of three gamma rays.

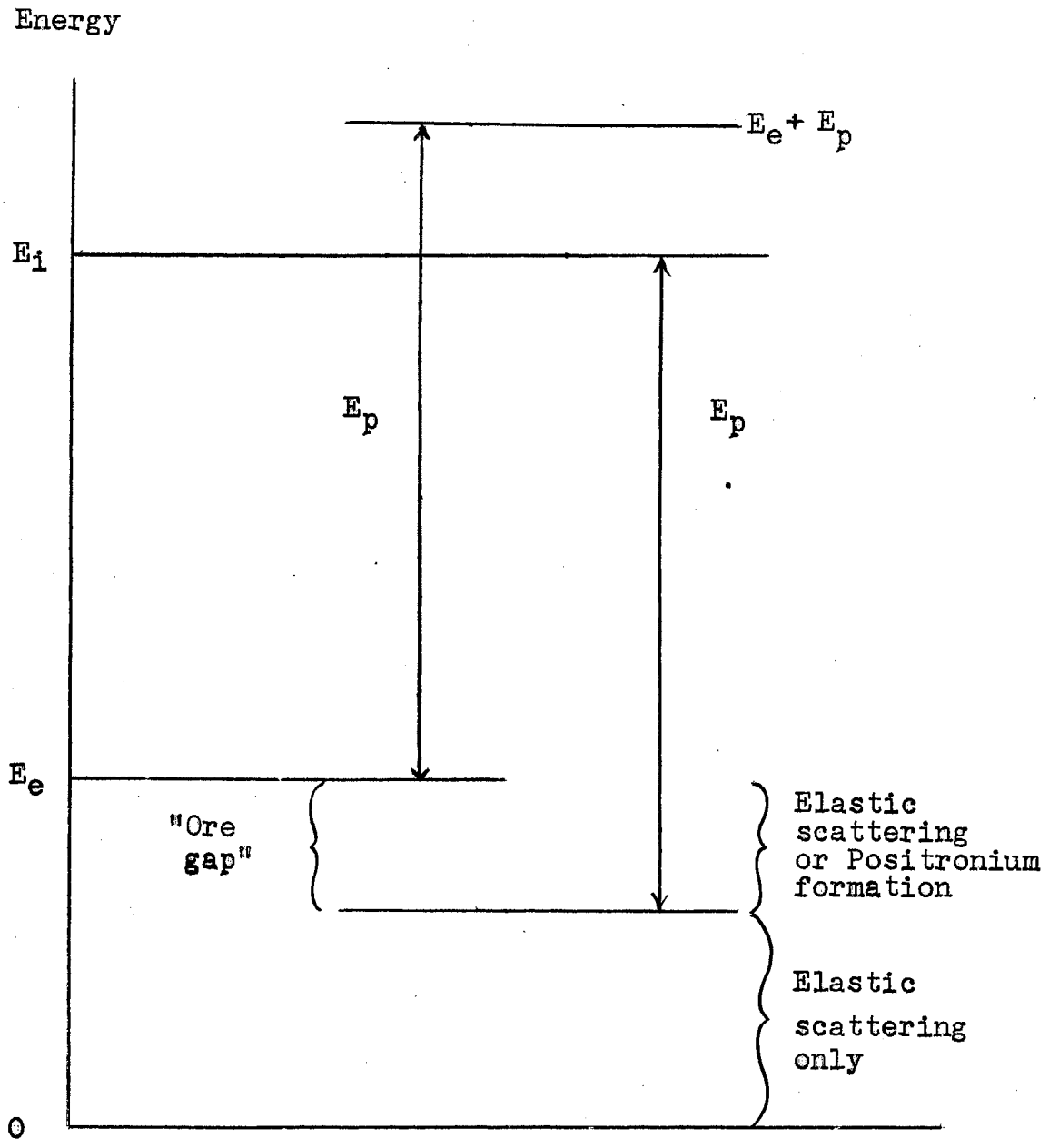

Figure 1. The "Ore Gap" (10)

To show that the singlet state cannot annihilate into an odd number of gamma rays, the principle of charge conjugation is used. For the case of an electron - positron pair the charge conjugation operator serves to exchange the charges and is equivalent to taking the product of parity and spin exchange for the system. The relative intrinsic parity of an electron and a positron is odd, and the singlet state is odd with respect to spin exchange, so the singlet state is even with respect to charge conjugation. The charge conjugation operator commutes with the total Hamiltonian and its eigenvalues are therefore constants of motion. The eigenvalue for states containing n quanta is $(-1)^n$. Thus for the singlet state, n must be an even number. It can be similarly shown that n must be an odd number for the triplet state. The two and three quanta annihilation of these states are the most probable.

An order of magnitude of the cross section for the two quantum annihilation of free particles can be gotten from a dimensional viewpoint (11). If the Coulomb attraction is neglected, the probability of the transition to two gamma rays will be proportional to e^4, the fourth power of the electronic charge. Taking relative velocities $v \ll c$, the transition probability will be independent of v and the cross section will vary as $\frac{1}{v}$. Then denoting the cross section by $\sigma_{2\gamma}$,

$$\sigma_{2\gamma} \approx \left(\frac{\alpha^2}{\beta}\right) f(\hbar, c, m) \qquad (4)$$

where

$$\alpha = \frac{e^2}{\hbar c} \quad , \quad \beta = \frac{v}{c} \quad . \tag{5}$$

The function f must have units of area, so (4) becomes

$$\sigma_{2\gamma} \approx \left(\frac{\alpha^2}{\beta}\right)\left(\frac{\hbar}{mc}\right)^2 = \frac{r_0^2 c}{v} \tag{6}$$

where

$$r_0 = \frac{e^2}{mc^2} = 2.8 \times 10^{-13} \text{ centimeter.} \tag{7}$$

A more rigorous derivation by Heitler (12) gives for the cross section

$$\sigma_{2\gamma} = \frac{\pi r_0^2}{\gamma+1}\left[\frac{\gamma^2+4\gamma+1}{\gamma^2-1}\ln\left(\gamma+\sqrt{\gamma^2-1}\right) - \frac{\gamma+3}{\sqrt{\gamma^2-1}}\right] \tag{8}$$

where

$$\gamma = \frac{E_+'}{\mu}, \tag{9}$$

E_+' is the total positron energy, and μ is mc^2, the rest energy. As γ approaches one, (8) becomes

$$\sigma_{2\gamma} = \frac{\pi r_0^2 c}{v} \quad . \tag{10}$$

This result represents an average over the four possible spin states of the two particle system. But two quantum annihilation only occurs in the singlet state, so

$$^3\sigma_{2\gamma} = 0 \quad , \quad ^1\sigma_{2\gamma} = 4\sigma_{2\gamma} . \tag{11}$$

Including the Coulomb attraction causes a distortion of the wave function, bringing the electron and positron closer to each other. The transition rate is proportional to the probability of finding the positron at the electron, so the above cross sections must be multiplied by the square of a normalized Coulomb wave function, evaluated at a distance of zero between the positron and electron. For positronium's bound negative energy states this factor is

$$|\psi(0)|^2 = \frac{1}{\pi}(2n a_0)^{-3} \tag{12}$$

(S state) with n being the total quantum number and

$$a_0 = \frac{r_0}{\alpha^2} \tag{13}$$

is the Bohr radius again. Then the mean lives, ${}^1\tau_{2\gamma}$, of the ${}^1S$ positronium states are

$$\frac{1}{{}^1\tau_{2\gamma}} = {}^1\sigma_{2\gamma} v |\psi(0)|^2 = \frac{1}{2}\frac{\alpha^5}{n^3}\frac{mc^2}{\hbar} . \tag{14}$$

Substituting numerically, obtain

$${}^1\tau_{2\gamma} = 1.25 \times 10^{-10} n^3 \text{ second}. \tag{15}$$

As mentioned before, the most probable annihilation from the ${}^3S$ state is three quanta annihilation. For this process, for a given n, the calculation of Ore and Powell (13) gives

$$\frac{{}^1\tau_{2\gamma}}{{}^3\tau_{3\gamma}} = \left(\frac{4}{9\pi}\right)(\pi^2-9)\alpha = \frac{1}{1115} \approx \frac{\alpha}{8} . \tag{16}$$

Again putting in numbers,

$${}^3\tau_{3\gamma} = 1.4 \times 10^{-7} n^3 \text{ second}. \tag{17}$$

This is the expression for the mean lives of the ${}^3S$ positronium states. The result (16) shows that the ${}^1S$ state annihilates about 1,115 times faster than the corresponding ${}^3S$ state.

Taking the ratio of the spin averaged cross sections reveals the numbers of three quantum to two quantum events in collisions with statistically distributed spins. Thus,

$$\frac{\sigma_{3\gamma}}{\sigma_{2\gamma}} = \frac{3/4\ {}^3\sigma_{3\gamma}}{1/4\ {}^1\sigma_{2\gamma}} = 3\left(\frac{{}^1\tau_{2\gamma}}{{}^3\tau_{3\gamma}}\right) = \frac{1}{372} \tag{18}$$

or

$$\sigma_{3\gamma} = \left(\frac{4}{3}\right)(\pi^2-9)\alpha r_0^2 c/v. \tag{19}$$

The Anomalous Lifetime Component

In one of the earliest experiments on positron lifetimes

in solids and liquids, Bell and Graham (14) found that some substances show only a short lifetime of about 1 or 2 x 10^{-10} second due to direct annihilation of the positron with an electron. Other materials, however, that could be classified as "molecular", showed in addition to the short lifetime a longer mean lifetime that can be as long as 3.5 x 10^{-9} second. These lifetime components are referred to as the τ_1 and τ_2 components, respectively. The τ_2 component, because of its unexpected appearance, is also referred to as the anomalous component. The intensity of each component changed from material to material.

A classification system for materials has been devised wherein those materials exhibiting the τ_1 component are classified as Type A, and τ_2 materials are classified as Type B. A generalization made by Wallace (9) as to the structure of the two types of materials is that free electrons range through the entire crystal in Type A materials, whereas electron exchange takes place only within individual molecules in Type B materials. Covalent forces present between molecules of the latter type are repulsive.

Some of the substances exhibiting the τ_1 lifetime in the Bell and Graham experiment were aluminum and other metals, the three forms of carbon, crystalline NaCl and crystalline sulfur. Landes (15) has attributed the short lifetime in metals to polarization of the electron gas by the positron, which causes an electron density in the vicinity of the positron that is greater than the average density of the

gas. Most annihilations probably occur between positrons and free electrons from the conduction band, although it is possible that some core electrons may annihilate. In non-metallic crystals it is the negative ion centers that annihilate with positrons.

Those materials exhibiting τ_2 were all the forms of water and ice, plastic sulfur, polystyrene, polyethylene, and Teflon. The Teflon had the longest τ_2 at room temperature of any substance tested. It is also interesting to note that Ferguson and Lewis (16) did not find the longer lifetime component in plastic sulfur.

The explanation of the τ_2 component as put forth by Bell and Graham and expanded upon by Ferrell (8) is this: the positrons enter the material, slow down, and form triplet positronium in about one-third of the cases. Then a process occurs which has been called "pickoff" annihilation. The positrons annihilate by two quantum emission with atomic electrons of the proper spin orientation. The probability of this process should depend on the density since it also depends on the amount of overlap of the positron and electron wave functions.

Bell and Graham noted that the value of τ_2 varied with the temperature of the material in which annihilation took place. This lifetime increased with increasing temperature, which is just opposite to what would be expected. The intensity of the τ_2 component did not seem to change with

temperature. The value of τ_2 for Teflon as measured by these experimenters ranged from 3.5×10^{-9} second at 20°C to 1.6×10^{-9} second at -196°C.

The variation of τ_2 with temperature for Teflon appeared to be linear until Landes, Berko, and Zuchelli (17) carried the measurements down to liquid helium temperatures. Their result of $\tau_2 = 2.0 \pm 0.2 \times 10^{-9}$ second at 4.2°K showed a large deviation from linearity.

Lundholm, Bjorkland, and Menius (18) measured the long lifetime component in Lucite, polyethylene, polystyrene, and nylon as well as Teflon in the range 25°C to 200°C. Their results showed that τ_2 varied directly with the absolute temperature.

A measurement of the variation of the three quantum decay rate in Teflon as a function of temperature was carried out by Graham and Stewart (19). Their data showed a greater triple rate in substances with a τ_2 component. They also found a correlation between the dependence of τ_2 upon temperature and the dependence of the three quantum rate upon temperature.

The τ_2 component undergoes great changes at the phase points of materials. Berko and Hereford (20) describe an experiment in which annihilation occurs in a melting naphthalene crystal. The melting point of this crystal is 80.1°C. The lifetime changed drastically across the phase point from about 1.2×10^{-9} second to almost 3.0×10^{-9}

second. The intensity of the τ_2 component also changed from about ten percent below melting to about thirty percent in the liquid phase.

Another group of materials that has drawn some interest in the positron lifetime field is the superconducting metals. Shafroth and Marcus (21) studied two quantum annihilation radiation from positrons stopping in lead at $4.2^{\circ}K$. alternately in a magnetic field of 750 gauss and with no field. The lead was then alternately in its normal state and in its superconducting state. Differences in the two quantum coincidence rate would indicate an enhancement of the three quantum radiation when the lead was superconducting. They observed no such difference in counting rate from superconducting to normal state. No change between the lifetimes in pure lead, commercial lead, and vanadium were observed in the normal and superconducting states by Graham, Paul and Henshaw (22).

Lifetime measurements have been made in liquid helium itself by Paul and Graham (23) and Wackerle and Stump (24). Three components of lifetime were found, and were attributed to parapositronium, free positron annihilation, and orthopositronium.

The Density Effect

Since the work of Bell and Graham, certain experiments and suggestions seem to favor the idea that the temperature effect is in reality a density effect.

In an experiment carried out by Stump (25), the lifetime of positrons was measured in water, Lucite, Teflon, and polyethylene at pressures up to 60,000 pounds per square inch. In both Teflon and polyethylene a marked decrease in τ_2 was seen with increasing pressure. The decrease in τ_2 was roughly proportional to the volume change. Stump proposed that the temperature variation of τ_2 is mainly the result of the variation in density, since varying the density by pressure gives comparable lifetime changes.

Wallace (26,9) suggested that the temperature effect results from thermal agitation, which produces density fluctuations, or "holes" between the atoms or molecules of a solid. Because of a repulsive exchange force, for any instantaneous configuration of the solid the positronium atoms tend to concentrate in these "holes". This lowers their energy and their pickoff annihilation rate. If a positronium atom is in a "hole" formed between two atoms, it will leave this "hole" and seek another when the atoms move back together.

An experimental confirmation of the density effect came from de Zafra and Joyner (10), who tested angular correlation and peak count rate variations with temperature in Teflon, water, ice, quartz, and naphthalene. Their results also indicate that the temperature and phase change effects are explainable in terms of density. After the measurement of the peak rate in Teflon at the highest

temperature, they applied pressure to the sample by means of a mechanical press and found a large decrease in the peak rate at the same temperature.

This is evidence that the τ_2 intensity is varying with pressure, or density. Therefore the amount of positronium formed depends on the density. This can be explained in terms of the previously discussed "Ore gap". An increase in density of a material causes E_p, the positronium binding energy, to decrease due to contraction of the wave function. Therefore the width of the Ore gap and consequently the amount of positronium formed will decrease with increasing density.

Purpose of this Investigation

The positron is no longer just an odd particle that interests only nuclear physicists. As Ferrell (8) has pointed out, it has become an experimental tool. It not only gives information about the mechanism of annihilation, but when it penetrates into a material and becomes an integral part of the electronic system, it "sends back" information about the structure of the sample via its annihilation gamma rays. The distortion of the internal structure due to the presence of the positron must be taken into account in interpretations of the data. Important conclusions are being made about the structure of metals, crystals, polymers, and other materials from such information. This process may also work in the other direction. If the

structure and properties of a material are well known, then annihilation data can be interpreted in terms of this knowledge.

In this experiment the lifetime of positrons in certain solids was studied as a function of temperature. This was done as a means of correlating lifetime and density, in those temperature regions where the density or related properties were known. In those regions where they were not known, properties of the solids were inferred from the lifetime data. Theoretical free volume calculations of the lifetimes were also compared to the experimental results.

The plastics polystyrene and Lucite were chosen as samples for positron annihilation because they exhibit the anomalous lifetime component. They are not unfamiliar materials in experiments of this type, but the variation of their τ_2 component was studied in temperature ranges in which little work has been done thus far; -196.5° C to 122.0° C for polystyrene, and -196.5° C to 23.7° C for Lucite. Also included in the results and interpretations are measurements by a colleague in a third plastic, polyethylene, from -196.5° C to 23.7° C.

Amorphous sulfur was studied at room temperature in an attempt to determine the presence of a long lifetime, and stannic oxide was studied in two forms, crystalline and powdered, to test the effect of the form of a solid.

CHAPTER II

APPARATUS AND PROCEDURE

The Circuit

The isotope Na^{22}, with a half life of 2.6 years, decays by emission of positrons with a maximum energy of 0.54 Mev. The Na^{22} decay scheme appears in Figure 2. In more than ninety-nine percent of the cases the decay is to an excited state of Ne^{22} with a half life of 4.8×10^{-12} second. The excited state decays to the ground state with the emission of a 1.28 Mev gamma ray. It is this prompt gamma ray, whose detection is used to signify the creation of a positron, that makes the isotope Na^{22} desirable as the positron source for this experiment. The detection of a 0.51 Mev annihilation gamma ray signifies the destruction of a positron. The mean life of the positrons emitted is the sum of the times of existence of all the positrons divided by the number emitted.

For measuring positron lifetimes, or other time intervals in the same range, one of two types of circuits is usually empolyed. One is the delayed coincidence circuit, in which a coincidence is counted when voltage pulses from two detectors arrive within a short time interval of each other. This time interval is called the resolution time of the circuit.

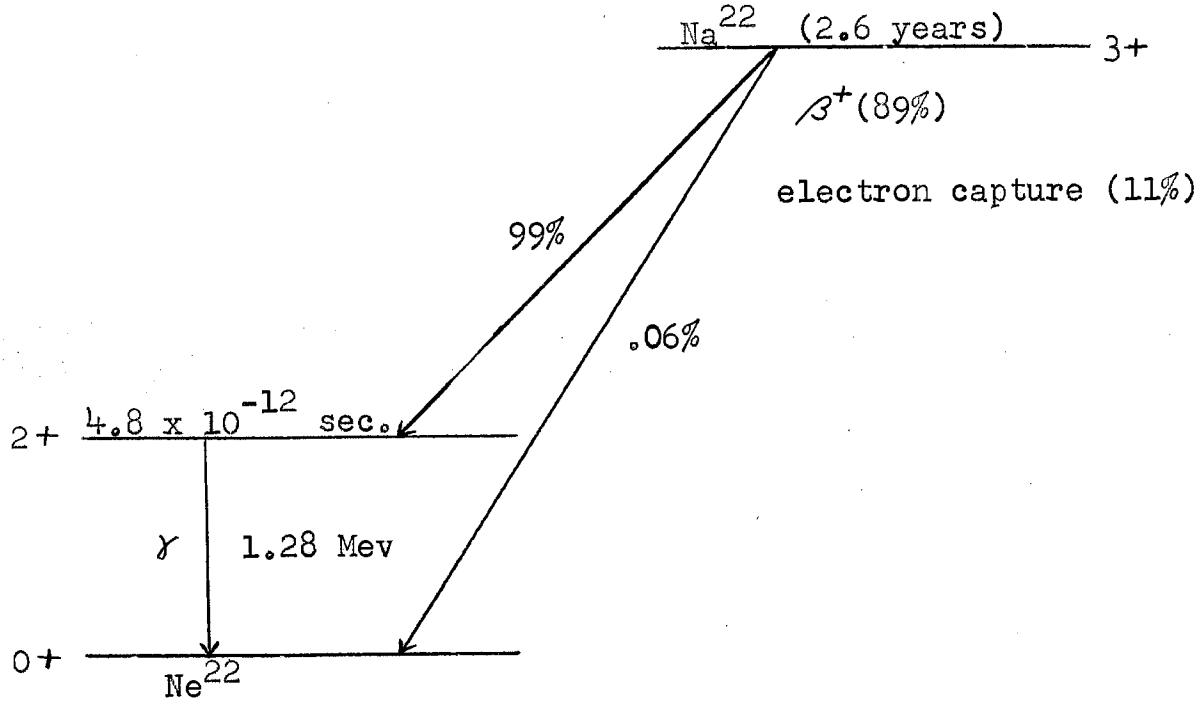

Figure 2. Na^{22} Decay Scheme

Coincidence count rates are plotted as a function of time delay inserted in one of the detector circuits. The other circuit contains a "time to pulse amplitude converter" which converts time intervals between pairs of input pulses into a pulse whose amplitude is proportional to this time interval. A multichannel pulse amplitude analyzer then can collect the data. Though this circuit is electronically more complex than the delayed coincidence circuit, data can be obtained faster and in a more readily interpreted form. This type of circuit was utilized in this experiment. Figure 3 shows the block diagram.

Scintillation counters using RCA 6342-A head-on photo-

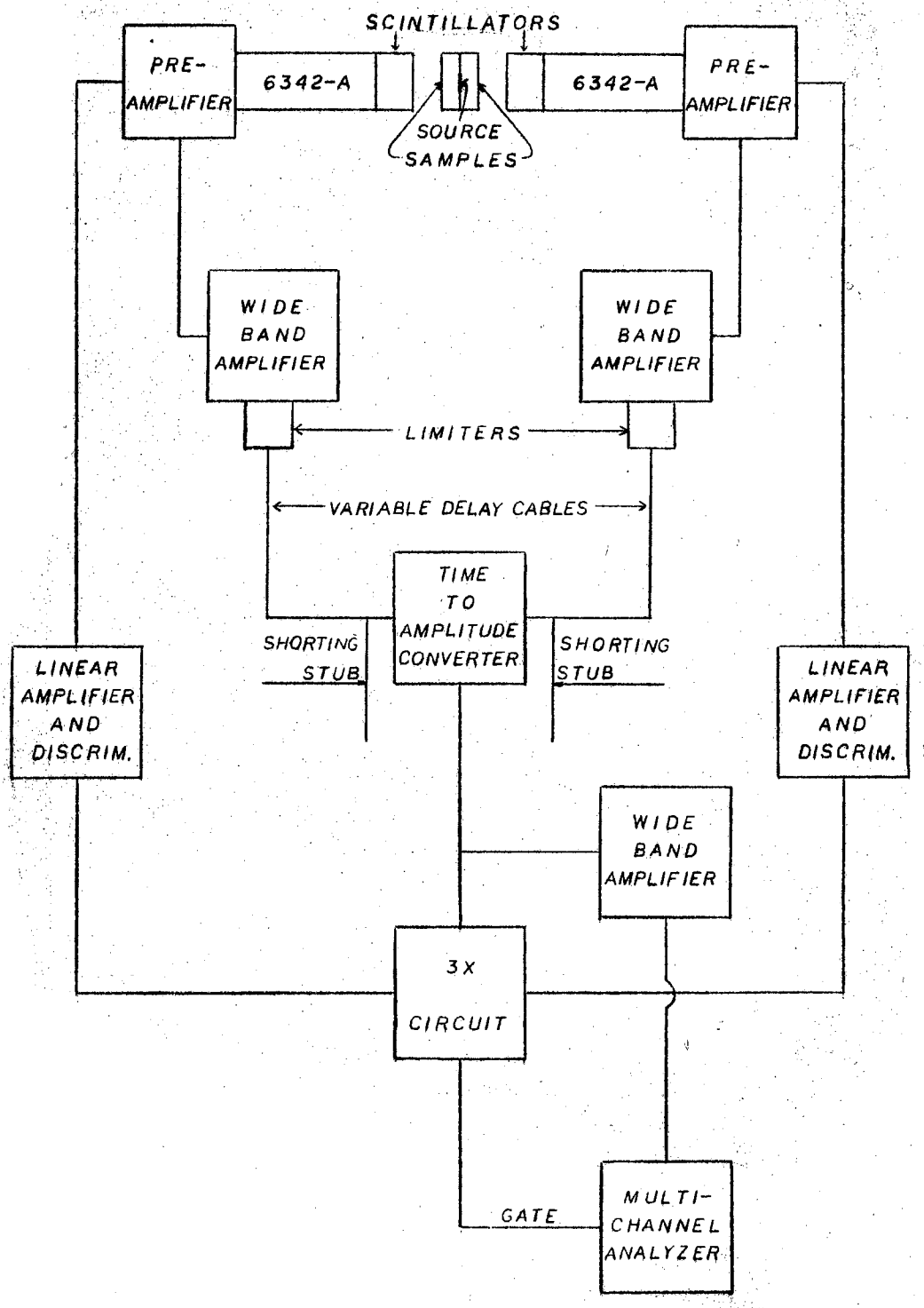

Figure 3. Block Diagram of the Circuit

multiplier tubes and plastic phosphors detected the gamma rays. Nuclear Enterprises NE160 plastic phosphors were chosen for their mechanical stability at temperatures up to 150°C; they were one inch in diameter and five-eighths inch thick. The decay time of these phosphors is 3.5×10^{-9} second. Polyvinyltoluene light pipes six inches in length and one inch in diameter connected the phosphors with the photomultipliers. This material is completely clear and colorless and has a refractive index and absorption band similar to that of the plastic. It was fastened to the face of the photomultiplier tube with Dow-Corning silicone QC-2-0057. Brass cylinders shielded the photomultiplier tubes, and a thin aluminum housing which screwed directly on to the brass cylinders covered the phosphors and light pipes.

About 1800 volts were supplied to the anodes of the photomultipliers by Hamner high voltage power supplies (Model N401). The negative pulses from the photomultiplier anodes were passed through preamplifiers and then by RG-114/U cable to Hewlett-Packard wide-band amplifiers (Model 460 AR) where they were further amplified.

Limiter circuits employing Western electric 404-A tubes were attached to the outputs of the wide-band amplifiers. The purpose of the limiters was to produce flat top pulses with short rise times of the same height in each detector circuit or channel regardless of whether the pulse was due to the detection of a 1.28 or 0.51 Mev gamma ray.

Pulses from the limiters were conveyed to clipping junctions by RG-7/U coaxial transmission cable, which has a characteristic impedance of 97 ohms. The clipping junctions consisted of 183 centimeter shorted RG-8/U coaxial cables. This cable has an impedance of fifty ohms. Pulse clipping was carried out in order that only the fastest rising part of the pulse was used and to get a resolving time less than the decay time of the phosphors. The cable length between the limiters and clipping junctions could be varied for time calibration of the time to amplitude converter.

The clipping junctions were connected directly to the time to amplitude converter. The converter circuit used was one designed by Simms (27). See Figure 4 for the circuit diagram. It shows all the biasing networks which are not discussed in the following brief description of the function of the circuit.

The input transistors T_1 and T_2 are conducting in the quiescent state, and the output transistor T_3 is cut off. If a positive pulse cuts off T_1 or T_2, all of the current flowing through R_1, which acts as a constant current source, is carried by the other transistor. When pulses arrive at both T_1 and T_2 within a time equal to the width of the pulses, both input transistors are cut off and the current goes into T_3. The current is integrated at the collector of T_3, which gives

$$V = I \Delta t / C_s^2 \qquad (20)$$

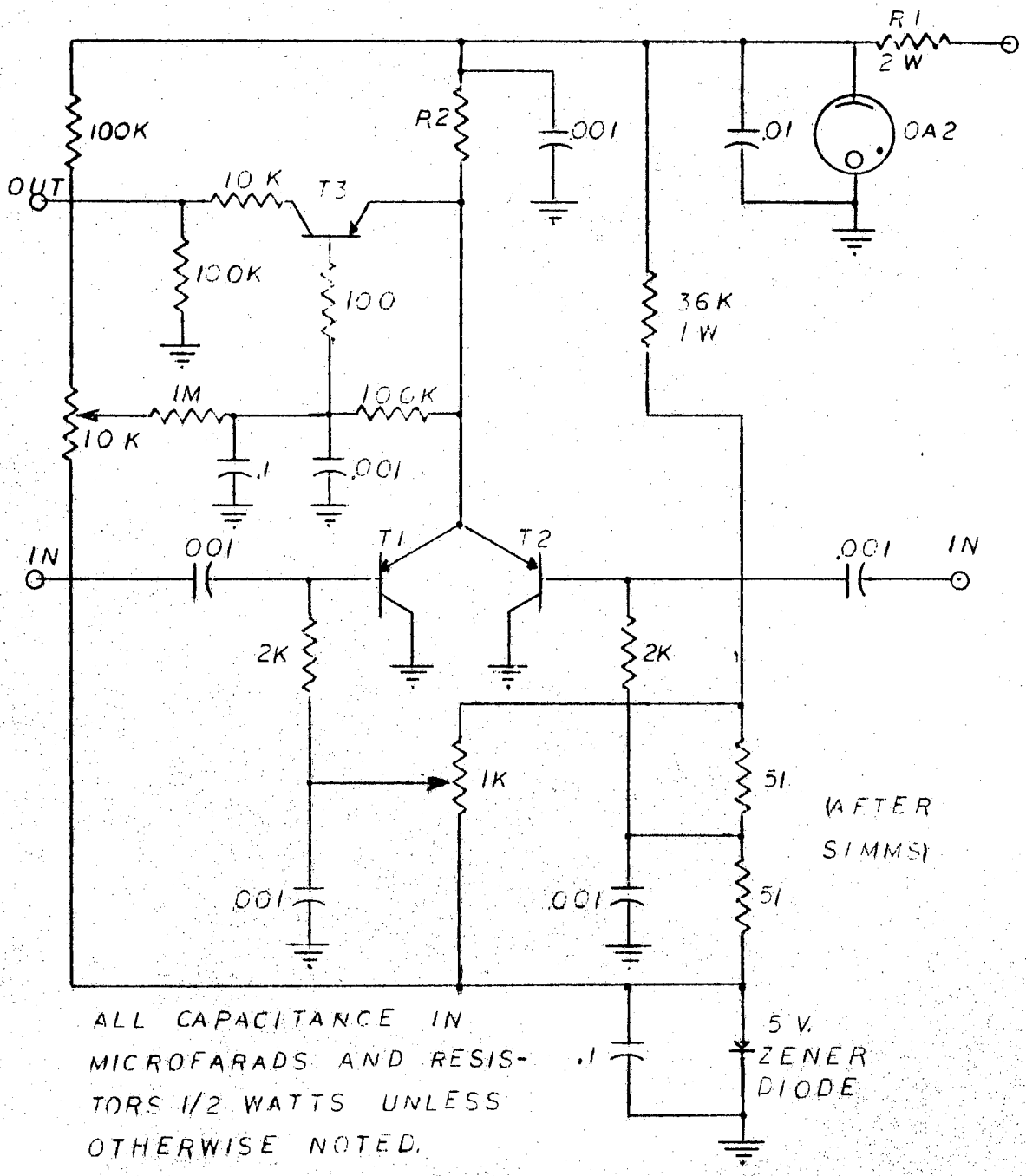

Figure 4. Circuit Diagram of the Time to Amplitude Converter (27)

for the amplitude of the output pulse where I is the current, C_s is the stray capacitance at the collector of T_3, and Δt is the period of time that both T_1 and T_2 are cut off.

The value of R_1 and the type of transistors used depends on the application of the system. Western Electric 2N1195 transistors were used for the lifetime measurements. The converter circuit will work with input pulses as small as 0.6 volt, but input pulses of one volt give the best time conversion (27).

The output pulses of the converter were fed into a Hewlett-Packard wide-band amplifier (Model 460 BR) and from there by RG 8/U cable to a Nuclear Data 512 Channel Data Reduction Analyzer (Model ND 130).

Energy discrimination was accomplished by passing positive pulses from the tenth dynodes of the photomultipliers to Baird-Atomic linear amplifiers (Model 215) with discriminators. One discriminator was set to pass only 1.28 Mev gamma pulses; the other was set to pass both 1.28 Mev and 0.51 Mev gamma pulses. This prevented false coincidences between two 0.51 Mev pulses being counted, but some coincidences between two 1.28 Mev gamma pulses were possible. However, the source strength was so low that these 1.28 Mev coincidences were very few. These two side channels then went into a triple coincidence circuit. The third input was taken from the time to amplitude converter. The triple coincidence circuit was a copy of the Advance Radiation Engineering Corporation Model 401 Coincidence-Anticoincidence Analyzer. The positive rectangular

output pulse of the triple coincidence circuit was then used to "gate" the multichannel analyzer; that is, the analyzer would not accept an output pulse from the converter unless it was told by the triple coincidence circuit that the event was a true coincidence. A true coincidence, then, was one in which the pulses had the correct energy in the side channels, and were separated in time by an amount such that, for given lengths of delay cable between the limiters and clipping junctions, there was some overlap at the time to amplitude converter, allowing an output pulse from that instrument.

In the analyzer, the pulse height of an input pulse from the time to amplitude converter is converted to channel number by an analog to digital converter. A count is then recorded in the proper channel. The data recorded by the analyzer can be displayed on an oscilloscope, typed out by an electronic typewriter, or plotted by an electronic X-Y recorder.

Calibration

Calibration of the instruments was carried out by recording the peak channels of time distribution curves of positron annihilation in aluminum for different delay cable lengths between the limiters and the clipping junctions. It is normally the centroids of the curves that are recorded, but the centroid varied from the peak channel by only a fraction of a channel for almost all curves. A plot of peak channel number versus inserted delay length in one detector circuit (i.e., delay length in one detector circuit minus

delay length in the other) was made. This plot, called the calibration curve, exhibits a linear portion; the reciprocal of the product of the slope of this line and the velocity in centimeters per millimicrosecond of a pulse in RG-7/U cable gives the calibration constant of the system in millimicroseconds, or nanoseconds, per channel. Figure 5 shows the calibration curve.

From the calibration curve, the range of linearity turns out to be ~ 8.45 nanoseconds. The range of linearity could be altered by changing the length of the shorting stubs.

The time resolution of the apparatus, which is the width of the aluminum time distribution curve at half maximum, was 1.6×10^{-9} second. Figure 6 is a typical aluminum curve of the apparatus, displaying the abovementioned resolution time. This curve was formed by plotting number of coincidences (counts) versus channel number, which has been converted to time. Since the centroid of the curve is shifted to the right by an amount equal to the lifetime of positrons in aluminum, the true zero of time was easily calculated.

Instrumental drift was evidenced by the shifting of the peak of a curve a certain number of channels over a certain amount of time. For this experiment, the drift did not amount to more than two channels over a twenty-four hour period. Since most of the data were taken in times that were short compared to twenty-four hours, it is reasonable to state that drift had little or no effect on the data. It was fortunate that most of the data were taken in an air

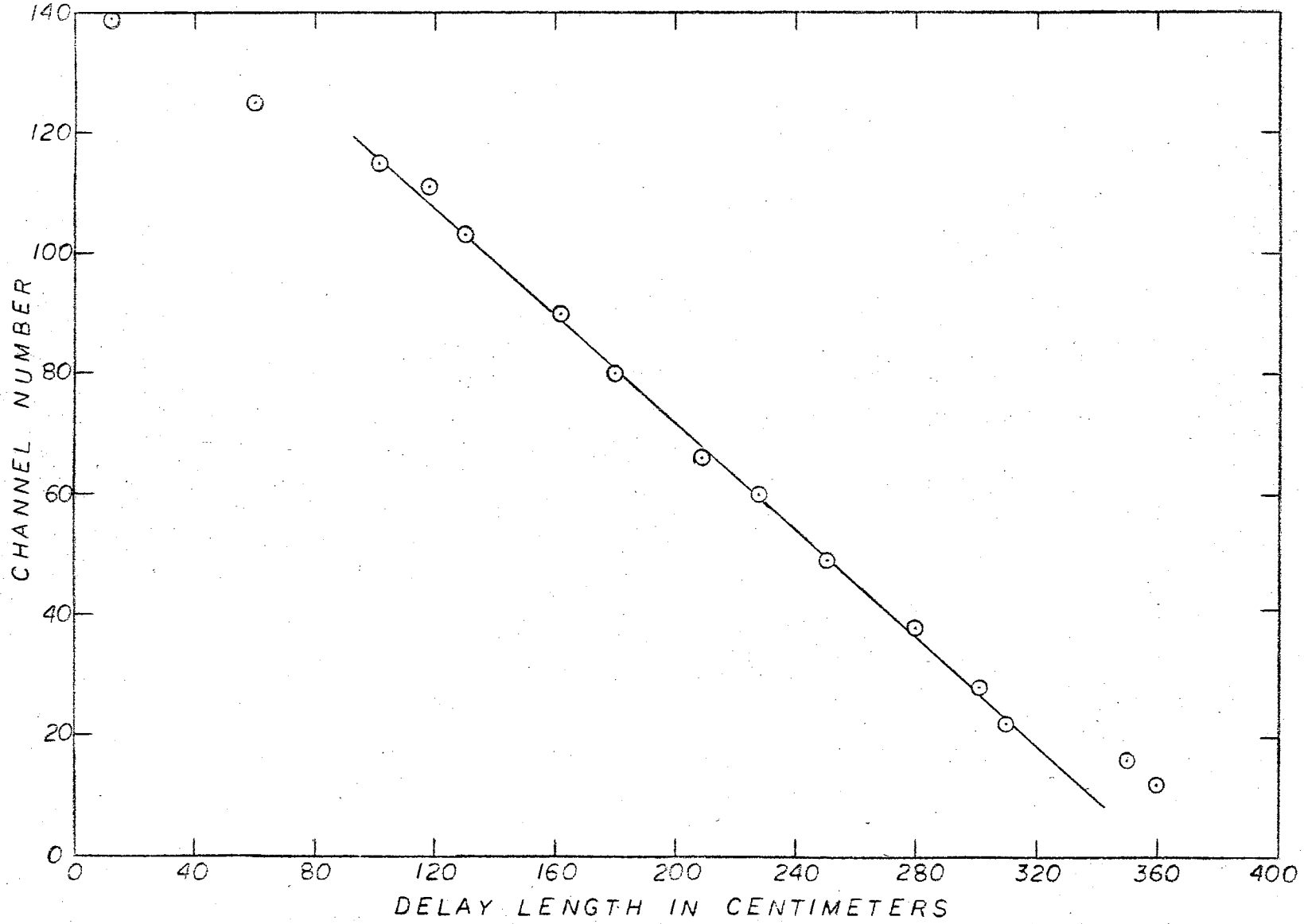

Figure 5. Apparatus Calibration Curve

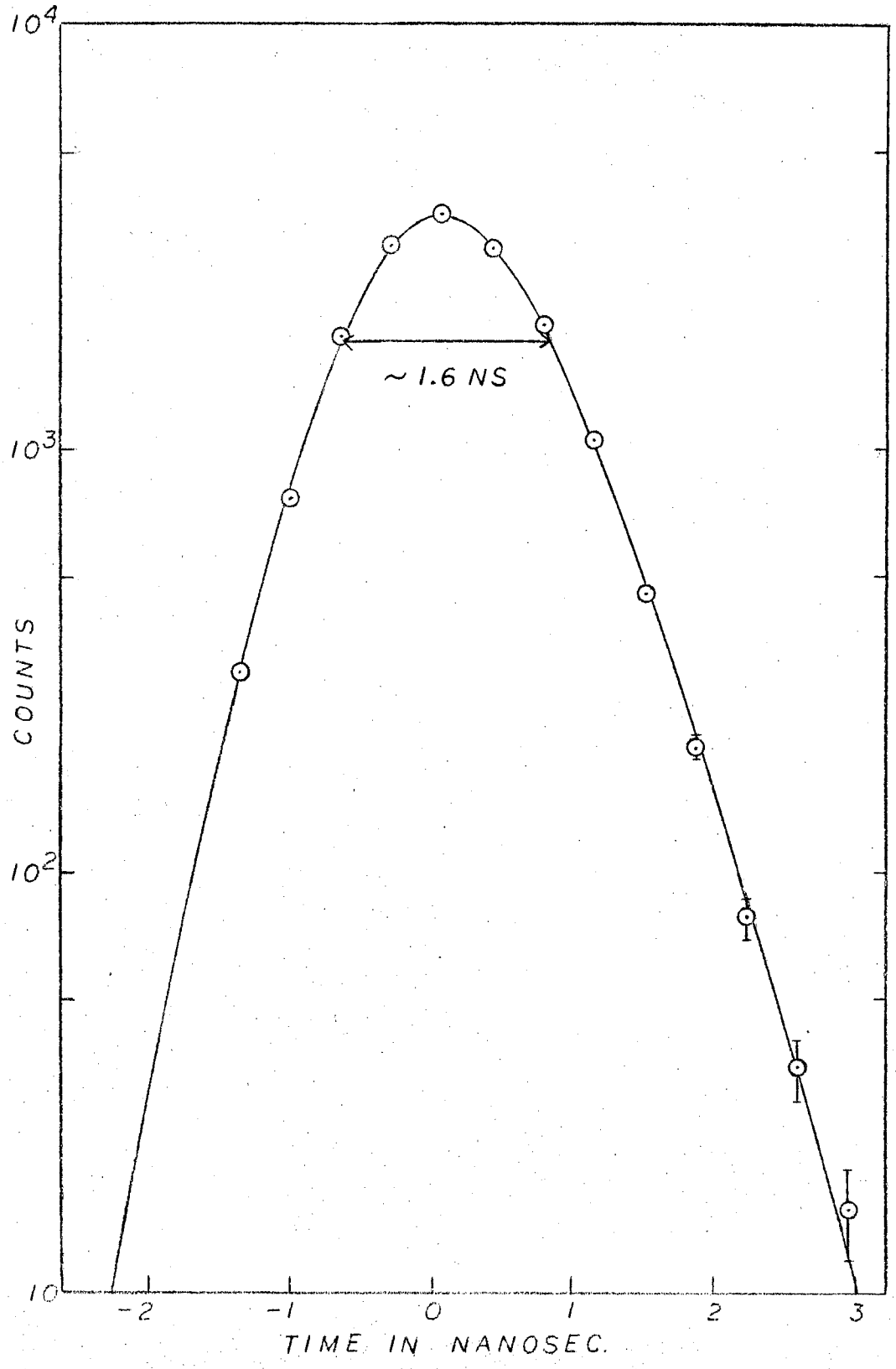

Figure 6. An Aluminum Time Resolution Curve
(The width at half maximum is the resolution time.)

conditioned room, where the temperature did not fluctuate more than one Centigrade degree. Large room temperature variations may be a cause of instrumental drift. The high voltage power supplies remained very stable throughout the experiment.

Preparation of Sources and Samples

Sources were deposited either on mylar or directly on the sample to be investigated. In the first case, ten microcuries of Na^{22} in a chloride solution were allowed to evaporate on a sheet of aluminized mylar 0.0002 inch thick. Another sheet of mylar was placed over the first, and then the sheets were stretched over an aluminum ring 1.25 inch in diameter. A second aluminum ring fitted onto the first in such a way that the mylar sheets were kept tightly stretched. Discs of aluminum or amorphous sulfur could be placed on each side of the source, forming a "sandwich", and the scintillators were pressed flush against the samples. In this way almost the entire solid angle was subtended by the scintillators. The discs were of more than sufficient thickness to stop all the positrons.

The amorphous sulfur samples were made by pouring molten sulfur into a small metal dish filled with water. After the irregularly shaped lump hardened, two discs 0.1 inch thick were machined from it. There is some danger of crystalline sulfur being formed in with the amorphous in this method.

Two stannic oxide crystals were obtained from the solid state research laboratory of this university. They had brownish-yellow discolorings, indicating the presence of a large number of impurity atoms, probably iron. They were 0.04 inch thick, and small enough in the other dimensions so that they could be taped to the mylar, completely covering the source. The stannic oxide powder used was commercially produced and contained only about 0.1% impurities. It was poured on both sides of a mylar covered source positioned in a small copper can. The copper can was placed directly between the scintillators for counting.

The plastic samples were made in cylindrical form, one inch long, and 0.438 inch in diameter. The polystyrene and Lucite samples were machined from commercially produced clear rods of these materials with approximate densities of 1.1 and 1.2 gm/cm^3 respectively. The polyethylene sample was made from a block of low density (0.92) polyethylene extruded in the Chemical Engineering Department of this university. The shape of the plastic samples is shown in Figure 7.

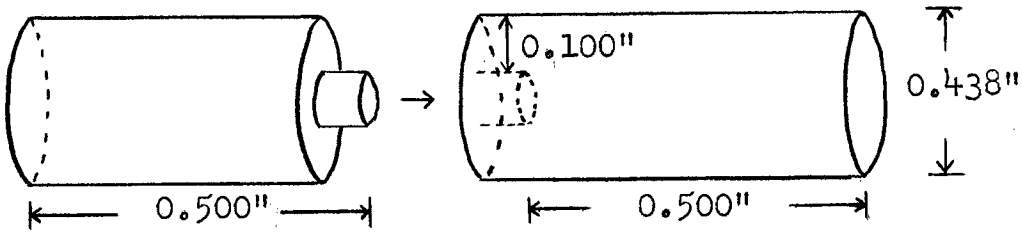

Figure 7. Shape and Dimensions of the Plastic Samples

Ten microcuries of the source were evaporated in the cutout section of each cylinder corresponding to the right hand portion of Figure 7. The other section of the cylinders corresponding to the left hand portion of Figure 7, made a force fit with the first section. In this way the plastic completely enclosed the source. The distance from the source to the ends of the cylinder was 0.500 inch, and from the source to the sides of the cylinder was 0.100 inch. These thicknesses were sufficient to stop all positrons. The cylinders were placed directly between the scintillators for counting.

The actual time necessary for a time distribution curve to accumulate to a given number of counts depended not only on the strength of the source, but also on the high voltage readings and on the discriminator settings of the non-overloading amplifiers in the energy side-channels. Increasing the discriminator settings insured against false coincidences being counted but increased the counting time, so that long range drift might affect the results. Almost all curves were allowed to accumulate to over 1,000 counts per channel in the peak. For an aluminum curve with 3,000 counts per channel in the peak, there were $\sim$ 54,000 counts total over all channels, representing the total number of positron annihilations recorded.

High and Low Temperature Apparatus

The low temperature data on the plastics were taken by placing the sample in a dewar flask that had a narrow flange in the bottom. The sample rested on the bottom of the flange, and liquid nitrogen, dry ice, or water and ice was poured in the dewar. The flange, and particularly the sample, was then centered between the scintillators. The outer thickness of the flange was 1.125 inch, and the inner dimension was 0.500 inch. A thermometer measurement of the ice and water mixture showed a temperature variation of not more than $\pm 0.5^{\circ}C$.

For the high temperature work, ohmic heating of the plastic samples was used by placing the samples in a copper rod wrapped with Chromel heating wire. The minimum length of wire to be used was calculated on the basis of a desired temperature of at least $300^{\circ}C$ for a rod thirty inches long and one inch in diameter, insulated by 0.25 inch of asbestos. This length turned out to be 33.6 inches of 26 gauge Chromel wire (0.214 ohms per inch).

A hole 0.500 inch in diameter was drilled completely through the rod twelve inches from one end. This hole accomodated copper cans with outside diameters of 0.500 inch, in which the cylindrical plastic samples were placed. The purpose of the cans was to keep the plastics from clogging the hole when they flowed and to prevent contamination of the rod due to diffusion of the source at higher temperatures.

Three feet of the heating wire was wrapped in coils five and one-half inches long, one and one-half inches on each side of the hole, forming two coils which were connected in parallel to a regulated voltage supply. Sauereisen cement insulated the wire from the rod. The entire rod was wrapped with asbestos tape to insulate against thermal radiation.

The plastic samples had 0.025 inch diameter holes drilled in them for thermocouples. An iron-constantan thermocouple and Leeds and Northrup K-2 potentiometer with standard cell and galvanometer were used to measure the temperature. After a sample reached thermal equilibrium, its temperature was checked every fifteen or thirty minutes. Although no temperature regulation device was used, the temperature varied only $\pm$ 2.0°C from the mean temperature. Appendix A gives some temperature regulation data for the rod.

While the length of the copper rod may seem inordinately long, its purpose will be detailed in suggestions for further experimentation in Chapter IV.

CHAPTER III

EXPERIMENTAL RESULTS

Data Techniques and Reduction

Data were allowed to accumulate until reasonable statistics were assured. Owing to the slightly different source strengths deposited on each sample, the accumulation times differed for each sample. Clock time was used to time a data run. Either immediately before, or immediately after each data run, an aluminum curve was taken. This provided a check on the stability of the apparatus, and was necessary for the calculation of the intensity of the anomalous lifetime component in the sample.

Each data run was typed out on the IBM electronic typewriter. Appendix B is a sample data sheet as typed out by the typewriter. It gives the number of coincidences in each channel. An averaging process was used to facilitate the interpretation of the data. It consisted of adding the number of coincidences in four consecutive channels, dividing the sum by four, subtracting background from this number, and considering the final result to be the number of coincidences in the second channel of the four. This process was carried out over all channels. Then these

averages were plotted on semi-logarithmic graph paper, with channel number as the abscissa, and number of counts or coincidences as the ordinate.

The background was determined by adding approximately 200 centimeters of delay cable to the 1.28 Mev gamma pulse channel, so as to count only accidental coincidences. The number of counts in a large number of channels (64 to 80) was then summed, and divided by the number of channels to obtain an average number of counts per channel. This figure, multiplied by a constant to allow for disparity in accumulation times, was subtracted from the four channel averages mentioned above. This technique was unnecessary in cases where the data curve covered only a small number of channels, and the background was evident from the typed-out data.

It was determined that this method of measuring the background does not take into account accidental coincidence due to photomultiplier noise and outside events such as cosmic rays. With the normal delay for data taking, and no source present between the scintillators, an eight hour count yielded less than a count an hour through the first 48 channels, nothing in the remaining channels. When the additional 200 centimeter delay was inserted and another eight hour count taken with no source, no coincidences were found. However, since the noise and outside events coincidences occured only in the first 48 channels, whereas most of the lifetime data curves extended over 128 channels, it was felt that nothing was lost in disregarding these

factors. Then the background that was subtracted from the data curves was due to coincidences between photons not related to the same positron.

The experimental time distribution curves are a composite of the apparatus resolution curve and the coincidence curves due to the annihilation of positrons in the samples. The anomalous lifetime component was recognized as being present in the plotted data by a "tail" or straight line that breaks off an otherwise bell shaped curve somewhere along its side. A straight line was fitted to the "tail" points by a weighted least squares method. The mean lifetime τ_2 is given by the product of the reciprocal of the slope of the straight line and the calibration constant. (See Appendix C).

The statistical uncertainty in τ_2 for each data run was found from the square root of the variance in the reciprocal of the slope, also discussed in Appendix C. If more than one data run was taken on a particular sample, each run yielding a lifetime and uncertainty of $A_i \pm a_i$, the most probable values of lifetime and uncertainty (28) were obtained from

$$\bar{A} = \sum_i \frac{1}{a_i^2} A_i \Big/ \sum_i \frac{1}{a_i^2} \qquad \bar{a} = \sqrt{1 \Big/ \sum_i \frac{1}{a_i^2}} \quad . \tag{21}$$

In order to separate the τ_2 component from the composite experimental curve, a "folding process", described in Appendix C, was carried out on each data run, or a representative data run if there was more than one for a particular sample at a given temperature. The intensity of

the τ_2 component, which is the percentage of positrons that annihilate by the "pickoff" mechanism, is the ratio of the area of the τ_2 component to the area of the composite curve. An alternate method of determining τ_2, that of the centroid shift of the area of the τ_2 component, was also used. This second method is somewhat cruder than the slope method, since the whole method is an approximate one, embodying Simpson's rule for the calculation of areas. The τ_1 component and lifetime value was found by subtracting the τ_2 component from the composite curve, and computing the centroid shift of the remaining τ_1 component. Throughout these calculations, the mean lifetime of positrons in aluminum was taken to be 1.9×10^{-10} second, as found by Bell and Jørgensen (29).

Experimental Lifetime Values

Table I presents a list of samples, the temperatures at which annihilation in them was studied, and the lifetimes and intensities obtained. The lifetime results in polystyrene at room and liquid nitrogen temperatures agree very well with those obtained by Bell and Graham (14),

$T = 20^{\circ}C$	$\tau_2 = 2.3 \pm 0.2 \times 10^{-9}$ second
$T = -196^{\circ}C$	$\tau_1 = 1.7 \pm 0.3 \times 10^{-9}$ second.

The intensities of the τ_2 components at these temperatures are found by the author to be about one-fourth lower than those quoted by Bell and Graham. The room temperature polystyrene value served as a check point, and this data

was rerun occasionally, as well as various points along the calibration curve, to make sure the calibration constant had not changed. The mean lifetime at 122°C takes an abrupt jump upward over values at lower temperatures. Figure 8 shows the time distribution curves for positron annihilation in polystyrene at the temperatures -196.5°C, 23.7°C, and 122.0°C.

The Lucite sample was tested only at low and room temperatures. The value of the mean lifetime at room temperature, $2.39 \pm 0.08 \times 10^{-9}$ second, differs markedly from the value obtained by Gerholm (30), $1.4 \pm 0.3 \times 10^{-9}$ second. However, there is reason to believe that the different properties of Lucites (also called plexiglass and perspex) made by different manufacturers, and the past history of these samples play some part in the value of the lifetime. Lucite time distribution curves at 23.7°C and -196.5°C are shown in Figure 9.

The polyethylene results reported in Table I were obtained by colleague J.L. Pigg (31) with the apparatus described in this thesis. They are listed here because of their relation to the measurements in the other polymers, polystyrene and Lucite. The room temperature value $2.60 \pm 0.06 \times 10^{-9}$ second is higher than the value found by Bell and Graham (14), $2.4 \pm 0.3 \times 10^{-9}$ second, but falls within their limits of error.

The amorphous sulfur results are interesting in that a plot of the data hints of a tail, in the region below

TABLE I

EXPERIMENTAL LIFETIME AND INTENSITY RESULTS

Substance	Temperature in Centigrade Degrees	$\tau_2 \times 10^{+9}$ Second (Slope Method)	$\tau_2 \times 10^{+9}$ Second (Centroid Shift)	$\tau_1 \times 10^{+10}$ Second	Intensity, I_2, in %
Polystyrene	-196.5	1.75 ± 0.06	1.6	1.4	22 ± 5
	- 78.5	2.10 ± 0.08	2.0	2.4	27 ± 5
	0	2.18 ± 0.06	2.1	2.9	28 ± 5
	23.7	2.32 ± 0.06	2.3	2.3	27 ± 5
	35.0	2.28 ± 0.09	2.2	3.2	31 ± 5
	44.6	2.41 ± 0.11	2.2	2.5	33 ± 5
	122.0	3.44 ± 0.20	3.0	3.5	40 ± 5
Lucite	-196.5	1.24 ± 0.06	1.2	1.1	23 ± 5
	- 78.5	1.52 ± 0.06	1.4	2.0	21 ± 5
	0	2.10 ± 0.12	1.9	2.4	13 ± 5
	23.7	2.39 ± 0.08	2.2	2.9	16 ± 5
Polyethylene (31)	-196.5	1.08 ± 0.15	1.1	2.3	23 ± 5
	- 78.5	1.27 ± 0.10	1.4	3.4	22 ± 5
	0	2.04 ± 0.10	1.9	2.7	12 ± 5
	23.7	2.60 ± 0.06	2.2	2.0	19 ± 5
Amorphous Sulfur	23.7	----	---	2.3 ± 0.2	---
Rhombic Sulfur (32)	23.7	----	---	2.3 ± 0.2	---
Stannic Oxide (Crystals)	23.7	----	---	1.7 ± 0.2	---
Powdered Stannic Oxide	23.7	----	---	2.2 ± 0.2	---

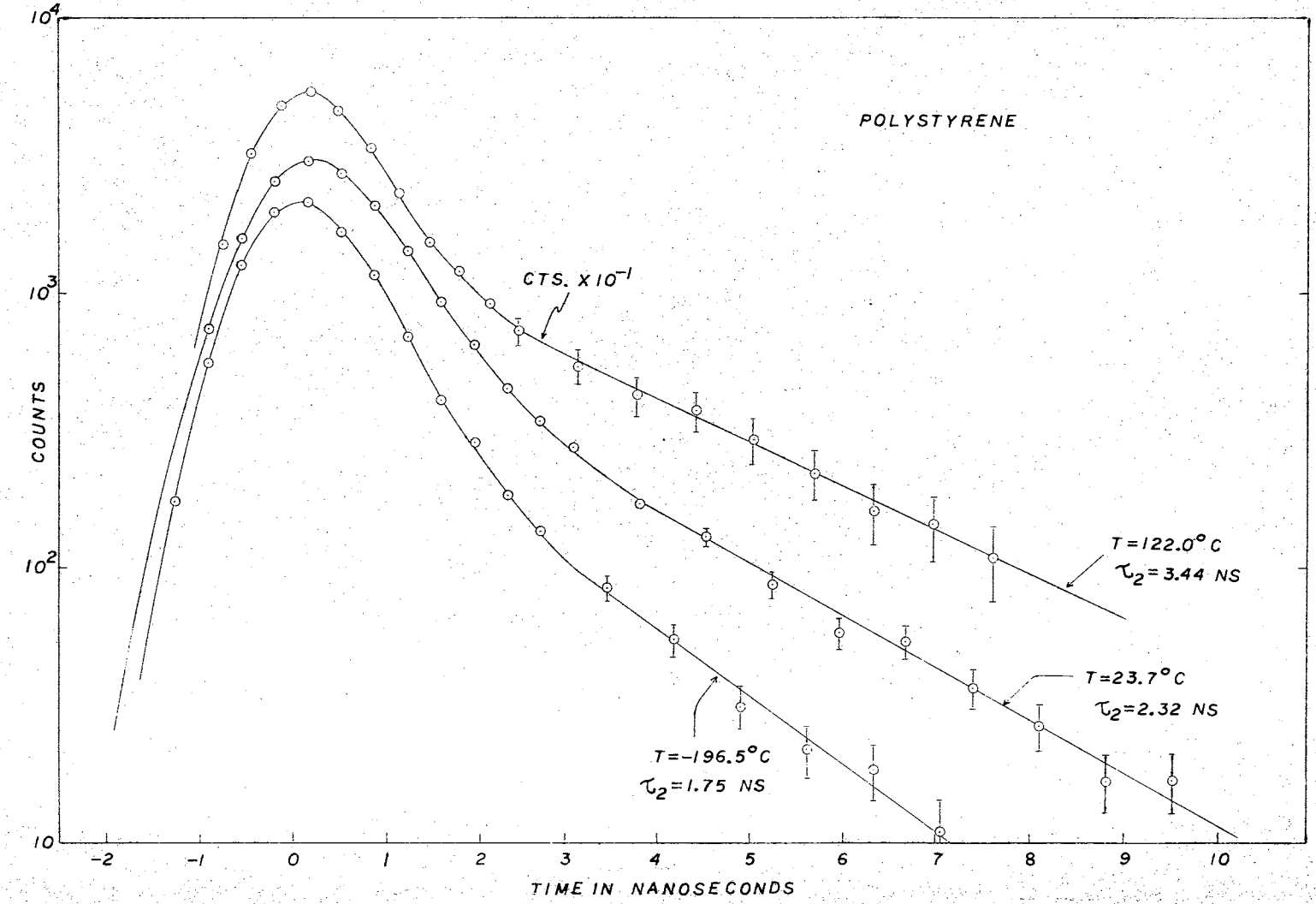

Figure 8. Time Distribution Curves for Positron Annihilation in Polystyrene at Three Temperatures (Vertical lines show standard deviation of points.)

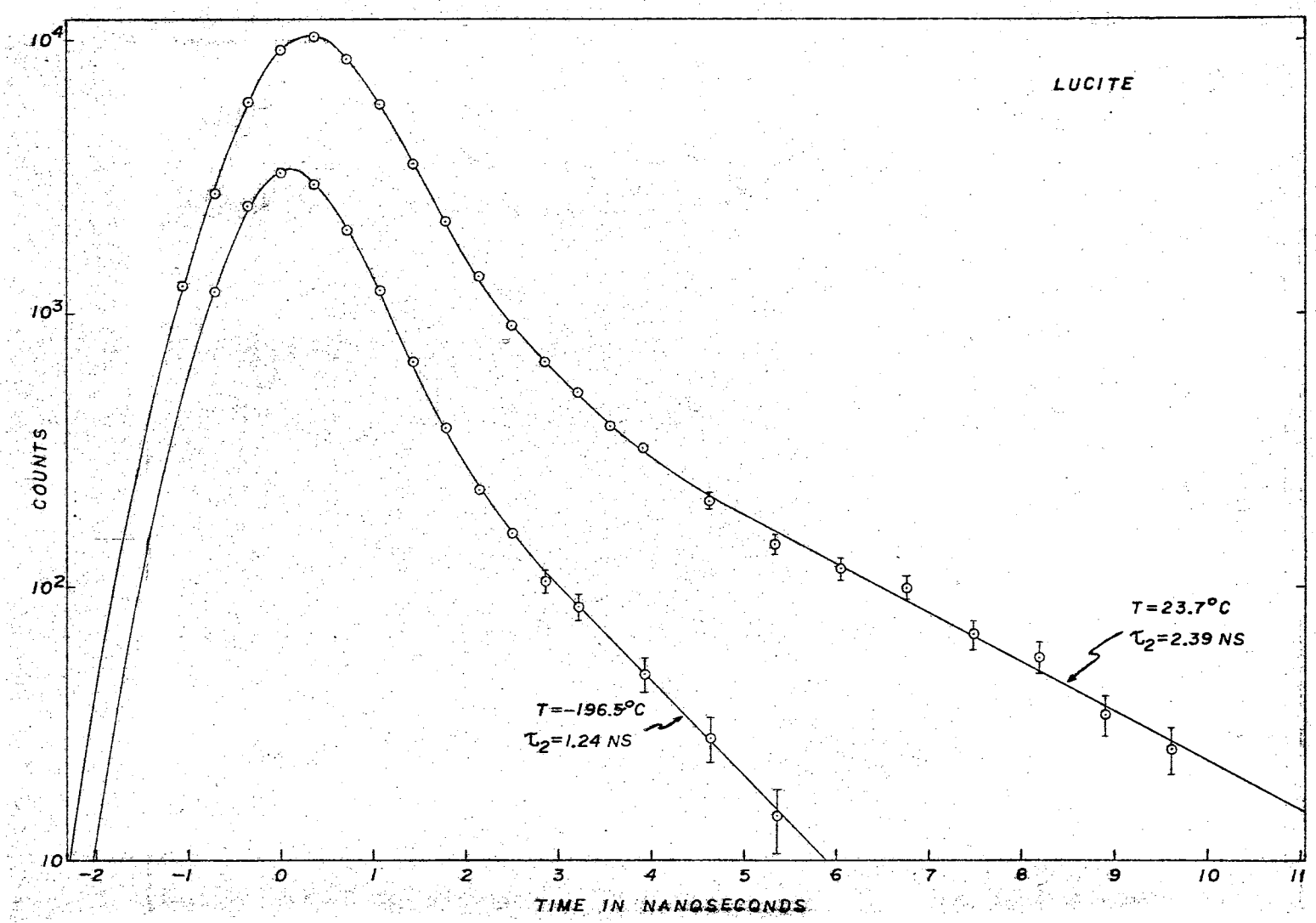

Figure 9. Time Distribution Curves for Positron Annihilation in Lucite at Two Temperatures
(Points of curves are representative; all points not shown.)

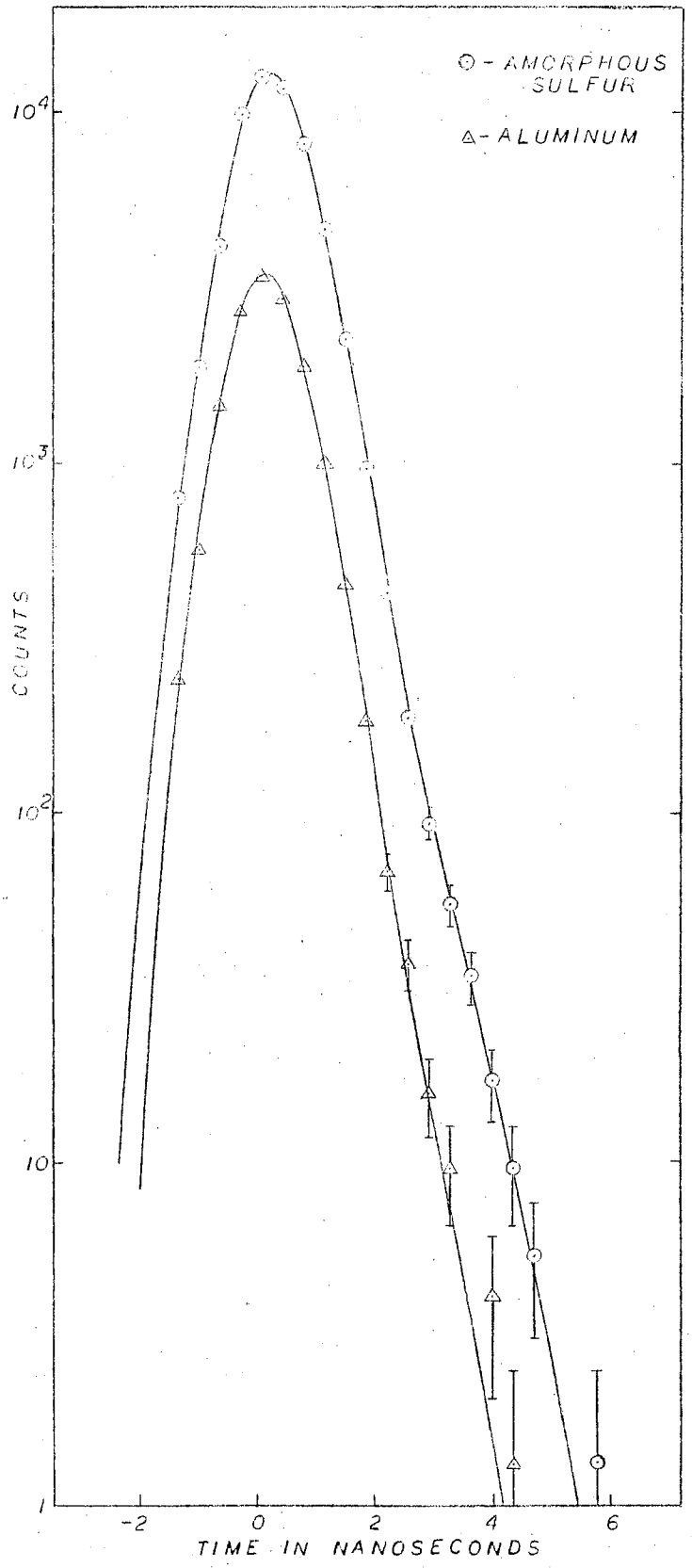

Figure 10. Time Distribution Curves for Positron Annihilation in Amorphous Sulfur and Aluminum at Room Temperature

about forty counts, with more than 12,000 counts in the peak (Figure 10). On the basis of the statistical uncertainty of the points below forty counts, it cannot definitely be said there is a τ_2 component in amorphous sulfur. If there is one, it does not exceed 6.9×10^{-10} second. Ferguson and Lewis (16) found no evidence for a τ_2 component greater than 8×10^{-10} second. But Bell and Graham (14) give

$$\tau_2 = 4.5 \times 10^{-10} \text{ second}$$
$$\tau_1 = 1.5 \times 10^{-10} \text{ second.}$$

The τ_1 listed in Table I for amorphous sulfur, $2.3 \pm 0.2 \times 10^{-10}$ second compares with those measured in monoclinic sulfur, $2.1 \pm 0.3 \times 10^{-10}$ second, by Bell and Graham (14), and in rhombic sulfur, $2.3 \pm 0.2 \times 10^{-10}$ second, by colleague R.D. Eagleton (32).

The stannic oxide crystals and powdered stannic oxide both exhibited only the short lifetime. The plotted data for them are similar in appearance to an aluminum curve.

The interpretation of all these data is discussed in Chapter IV.

Errors

The immediately recognizable and numerically determinable errors in this experiment are the statistical error in the fitting of straight lines to curves having the τ_2 component, and error in the instrumental calibration.

The first of these was computed by finding the square

root of the variance, or the standard deviation, of the reciprocal of the slope of the straight line, and multiplying it by the calibration constant. This method took into account the statistical uncertainty in the number of counts for each point.

To obtain the error in the calibration of the apparatus, the standard deviation of channel number about the calibration line was found. This value was added and subtracted to one end point of the line, while the other end point was held fixed. Then the slopes of the two lines defined by the new end points and the fixed end point determined the variation of the calibration constant. The largest variation of the calibration constant was 2.6 per cent, which had an almost negligible effect on the lifetimes.

These two errors were combined by taking the square root of the sum of their squares.

Errors that could not be precisely computed were also present. The largest contributor to this category was the background method. It is likely that background subtraction by the previously described method gave an error in one direction only. That is, either too much or not enough background was consistently subtracted. Other factors contributing to the error were fluctuations of the line voltage and room temperature, which affects photomultiplier tube gain. These factors probably showed up in the instrumental drift, which was not great; therefore they could not have been of importance.

The errors quoted in Table I for the τ_2's by the slope method includes only the computable statistical error, and not any estimated amount due to background, etc.

No errors are listed for the τ_2's by the centroid shift method, but it is reasonable that they should be larger than those for the slope method. The slope of the "tail" is a determining factor in the centroid shift process, so all the errors of the slope method are applicable to the centroid shift method. In addition, the approximations used in computing areas, and drift of the apparatus resolution curve contribute to the error. The errors in the τ_1's are large, but can only be estimated, and therefore are not listed. The errors in the intensities are estimated.

The error in τ_1 for those materials showing only that lifetime was arrived at by postulating a drift of two channels in the aluminum resolution curve, and calculating the lifetime under that condition. This was considered to give the maximum variation in τ_1. No estimated systematic error was added to this value.

The errors found for the τ_2's by the slope method are fairly small, except at higher temperatures in polystyrene. The values of τ_2 as calculated by the two methods agree as well as can be expected, differing by more than 0.2×10^{-9} second in only two cases.

Error can be reduced by numerous determinations of the lifetime in a particular sample and by extremely good regulation of high voltage power supplies, line voltage, and room temperature, so as to minimize instrumental drift.

CHAPTER IV

Polymers

Plastics are composed of large molecules built up by the repetition of small simple chemical units. Such molecules are called polymers, and this name is given to plastics in general. Polymers are crystalline if their molecular structure is chemically and geometrically regular. Regions of regularity extend over only a few hundred angstroms, however. Between the regular regions, irregular or amorphous regions occur. A polymer molecule is long enough to pass through several regions of both types. Some polymers are completely amorphous. Polystyrene is almost completely amorphous, and polyethylene is 60 to 70 per cent crystalline (33). Lucite is listed as being completely amorphous, but there is reason to believe that the sample used in this experiment was crystalline to some degree.

Crystalline polymers undergo a first order phase transition upon being heated to a certain temperature. This temperature, different for each polymer, marks the disappearance of the crystalline region, and is called the crystalline melting point, T_m. At this temperature the polymer becomes a liquid and exhibits discontinuous changes in density, heat capacity, and other properties. Completely

amorphous polymers do not have first order transitions.

Polymers also can have second order phase transitions, or glass transitions. Below the transition point, called the glass transition temperature, T_g, a polymer appears hard, brittle, and glassy; above it, the polymer becomes soft, flexible, and may flow if T_g is high enough. Changes in specific volume, or density occur again across the transition point (33,34).

A crystalline polymer then has two phase transitions, but the glass transition may have only slight effects since it is associated with the amorphous regions. Some transition temperature data from various sources are, polystyrene, $T_g \approx 80^{\circ}C$ (33,34,35); Lucite, $T_g \approx 57^{\circ}C$ to $68^{\circ}C$ (33,34); and polyethylene, $T_m \approx 112^{\circ}C$ (33,36), $T_g \approx -28^{\circ}C$ (37).

Below T_g, the polymer molecules become tightly packed and their mobility is small. As the temperature is lowered, the structure of a polymer does not change, but there is a small linear decrease of the volume, caused by further contraction of the molecular structure.

Upon plotting the values of mean lifetime against temperature for polystyrene, it was noted that a linear relationship from $-196.5^{\circ}C$ to $44.6^{\circ}C$ occurred. As mentioned above, there is also a linear relationship between specific volume, the reciprocal of the density, and temperature for polymers below the glass transition temperature. Curves of specific volume versus temperature for polystyrene were obtained (34,35), and these data were plotted on the same

graph with the lifetime data to a scale such that the line representing the variation of specific volume formed a good visual fit of the lifetime data points below T_g. This graph appears as Figure 11. Above T_g, the single lifetime data point does not lie on the line, but indicates that the lifetime may increase more sharply with temperature than does specific volume. There can be some flexibility in the specific volume curve above T_g depending on the molecular weight of the sample, but data seem to show (35) that the specific volume is independent of molecular weight below T_g. It must also be pointed out that one experimental point is not sufficient to accurately determine the lifetime variation above T_g.

The lifetime probably continues to increase with temperature above T_g as long as the specific volume increases. Some rather long lifetimes could then be expected. This behavior is different than that observed in naphthalene (38), where the lifetime remains fairly constant after the phase transition at 80°C. However, this is a crystal melting transition, and the density must also remain fairly constant above it. This is the case in polyethylene above its melting point, 112°C.

Figure 12 shows similar information for Lucite and polyethylene. The specific volume data for Lucite are uncertain at lower temperatures and this has been indicated on the figure where the line becomes dashed. If the line were to be extended to lower temperatures, the experimental

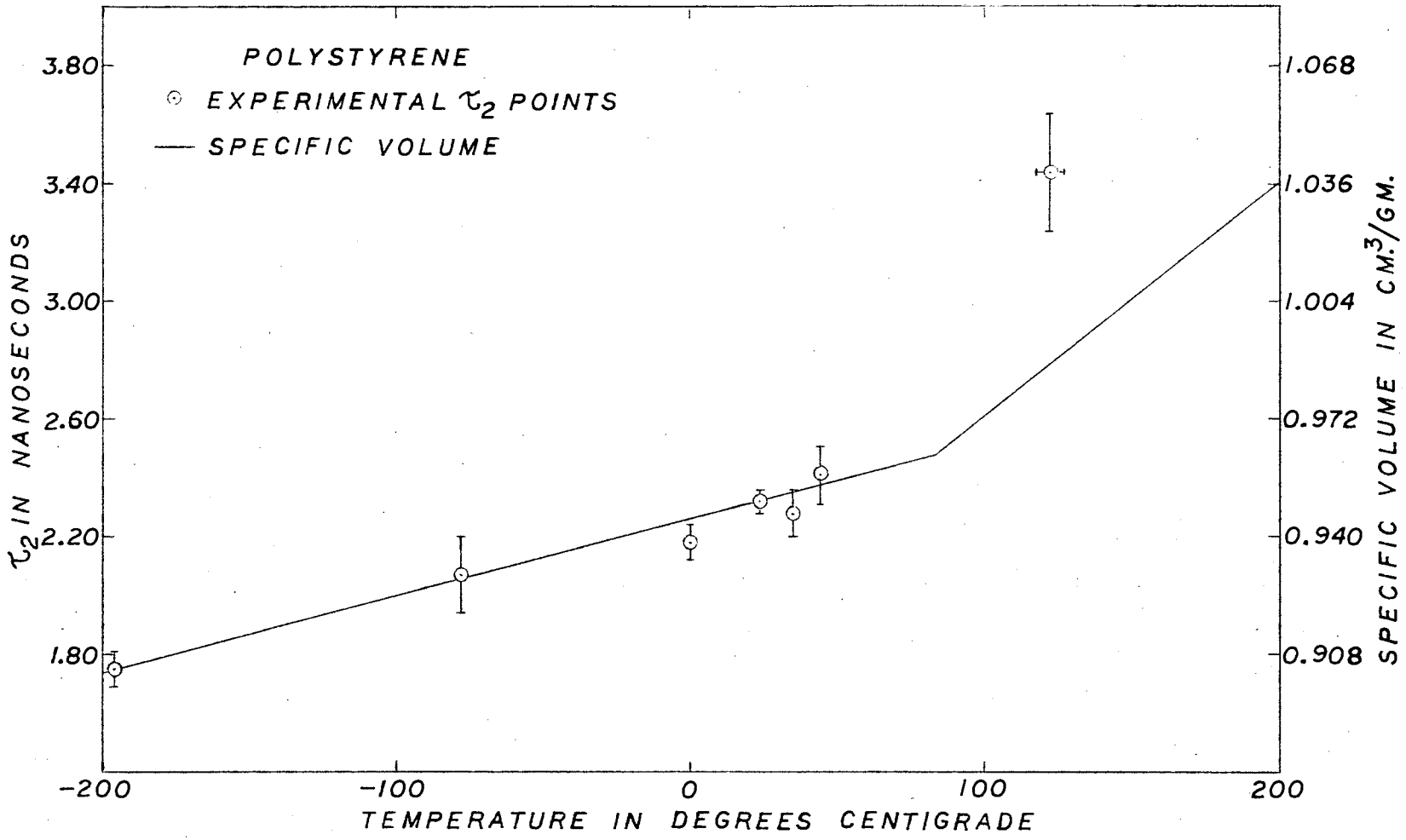

Figure 11. Experimental Positron Lifetime τ_2 and Specific Volume as a Function of Temperature for Polystyrene
(Vertical lines indicate statistical error in τ_2)

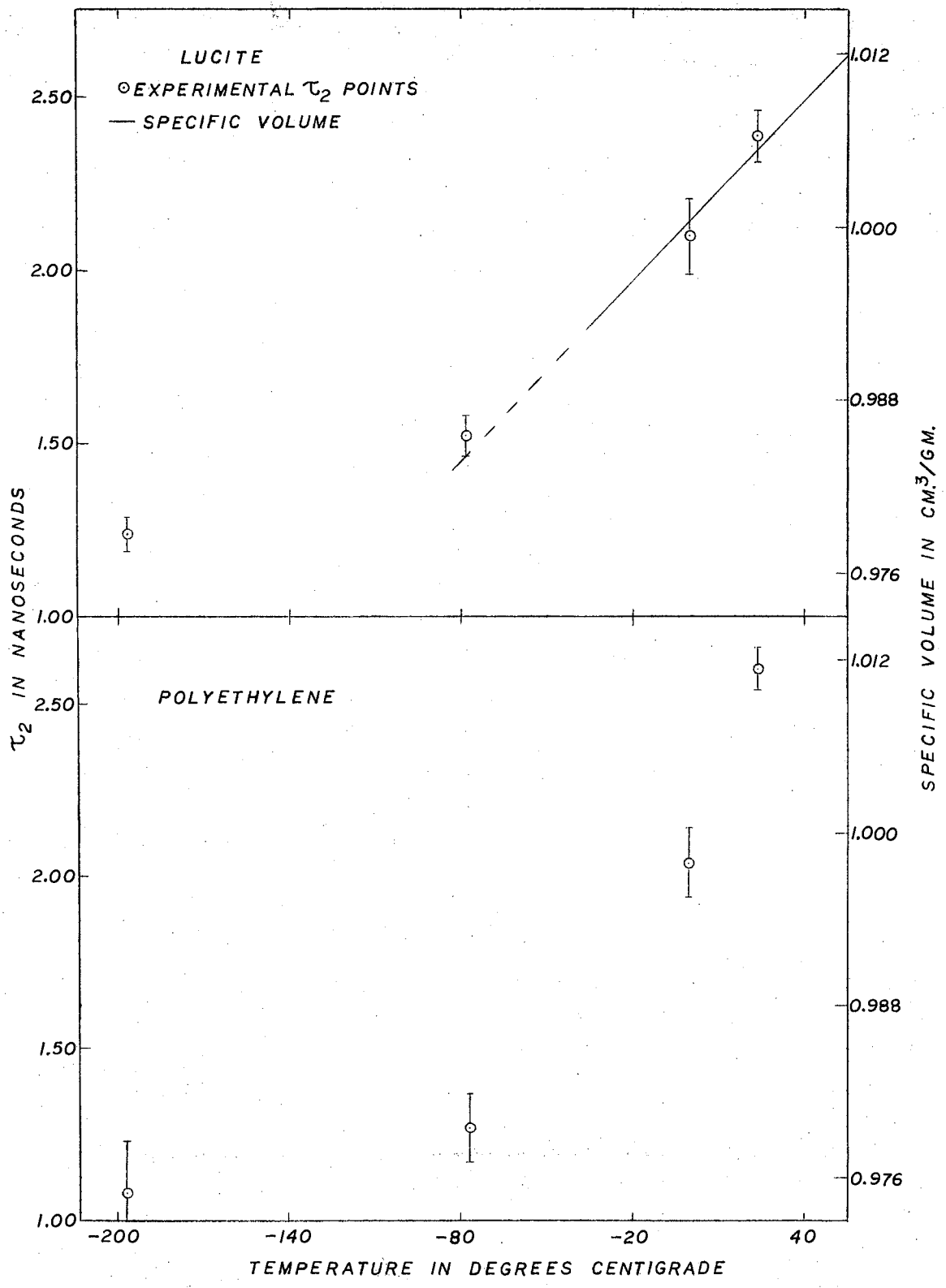

Figure 12. Experimental Positron Lifetime τ_2 and Specific Volume as a Function of Temperature for Lucite and Polyethylene

lifetime point at -196.5°C would not fall close to it. On the basis of the density effect, then, it appears that the particular Lucite sample used in this experiment has a discontinuous change in density at lower temperatures, similar to a phase transition. The temperature at which the change occurs could be about -100°C, or -40°C if the specific volume line is drawn to lie more directly along the two higher temperature points. In the second case, another line describing a slower change of specific volume with temperature would approximately be defined by the two lower temperature lifetime points.

The explanation of all this is either that the sample was originally partly crystalline, or that the lower temperatures have some unexplained effect on the material, causing denser packing of the chain molecules. The sample was hard and glassy at room temperature, so a low temperature transition was not expected from its appearance. The question should be resolved at higher temperatures, where the lifetime values will sharply increase at the transition, then remain constant above it if the sample is partly crystalline.

If straight lines are drawn through the two higher and the two lower temperature polyethylene lifetime points, the intersection of the two lines is at about -30°C, very close to the glass transition temperature of -28°C, at which abrupt changes are expected.

Figure 13 is a plot of intensity, I_2, versus temperature

for each of the three polymers. An increase in intensity at high temperatures, and a decrease at the lowest temperature with a constant region between was found for polystyrene. The intensity is related to the amount of positronium formed. If under one condition more positrons are forming positronium (instead of annihilating directly) than under a second condition, then more positrons can annihilate with a lifetime τ_2, and consequently the intensity I_2 will be greater for the first condition. At low temperatures, increased density causes a narrower Ore gap, and less positronium is formed. The reverse is true at high temperatures. This argument makes the temperature variation of intensity in polystyrene plausible. But then the data for Lucite and polyethylene are completely baffling, for the intensities at 0°C and room temperature are lower in these two substances than those at dry ice and liquid nitrogen temperatures. These results cannot be explained in terms of density alone. More must be known about the structures of these substances and the effects of phase transitions on the structures.

The intensities in these two substances are nearly equal at each temperature. This fact strengthens the argument for a partially crystalline Lucite sample, and makes a transition at -40°C more likely than one at -100°C. The intensities in another crystalline polymer, Teflon, are constant at $\sim$ 30% over this temperature range (14).

The τ_1 values for these polymers at the various temperatures show an almost random distribution. This is

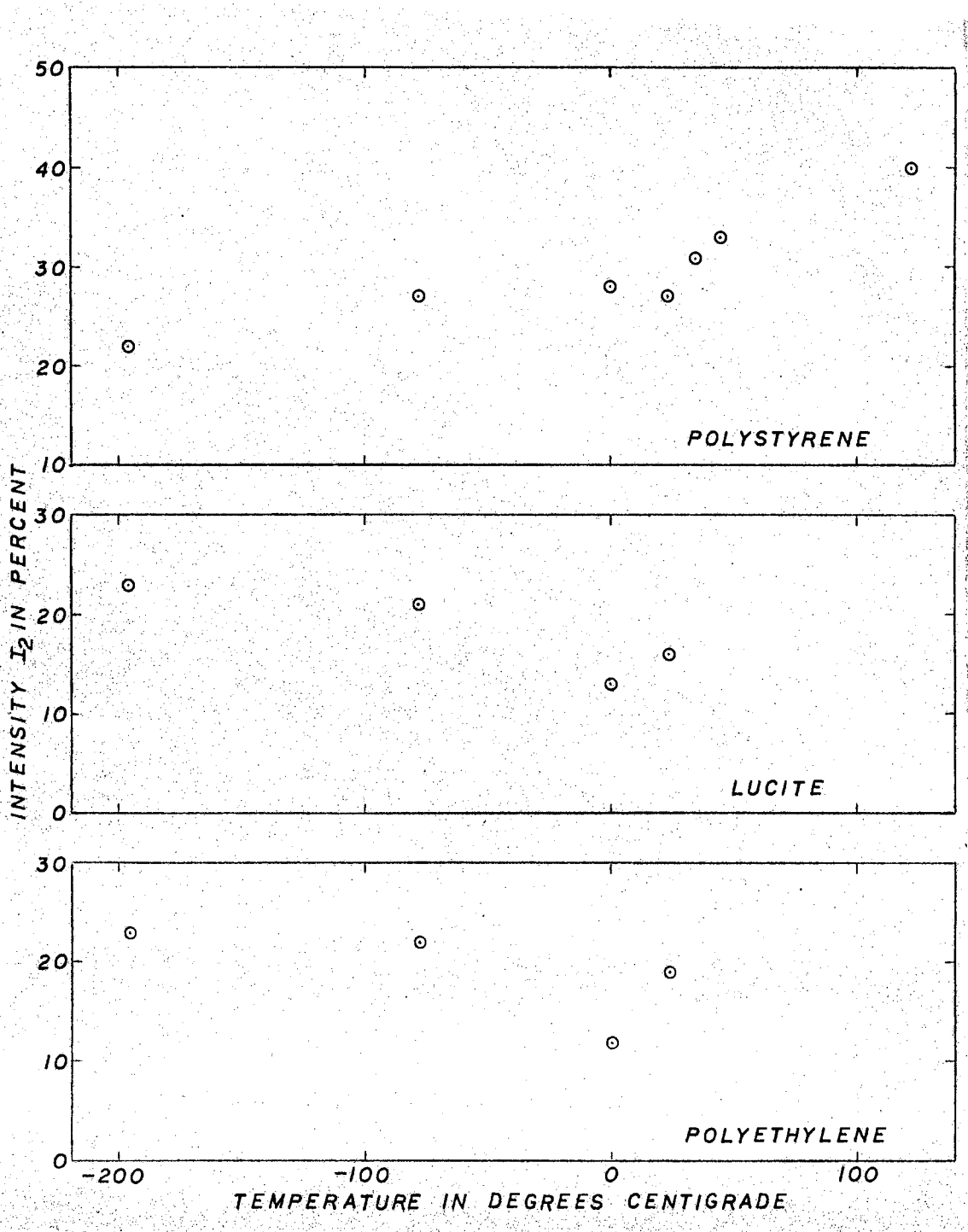

Figure 13. Intensity, I_2, Versus Temperature for the Three Polymers (All intensities are ± 5%.)

due to the approximate manner in which they are calculated. From equation (14), Chapter I, or the equivalent equation

$$\tau_1 = (\pi r_0^2 c \rho_0)^{-1} \tag{22}$$

where r_0 is the classical electron radius, and ρ_0 is the electron density, it is seen that temperature should have no effect on τ_1 for a particular sample.

In summarizing, it may be said that the variation of lifetime with temperature is in general agreement with the variation of specific volume with temperature, especially in polystyrene. Since the discussion thus far has been qualitative and concerned with a gross, over-all effect of temperature on the samples, exact agreement is not to be expected.

Free Volume Calculations

A more quantitative method of accounting for the increase of τ_2 with temperature, based on quantum mechanical ideas, has been devised (39).

In a molecular lattice, a thermalized positronium atom has a de Broglie wavelength two to three orders of magnitude larger than the dimensions of the "free volume" per molecule available to it. Pickoff then depends on the amount of overlap of positron and lattice wave functions. The electron pickoff rate, γ_p, in a lattice of electron density distribution $|\Psi_L(\vec{r})|^2$ composed of neutral molecules with closed shells may be written

$$\gamma_p = \pi r_e^2 c \int_L \Psi_L^*(\vec{r}) \Psi_{s+}^*(\vec{r}) \Psi_{s+}(\vec{r}) \Psi_L(\vec{r}) \, d^3\vec{r} \tag{23}$$

where $\Psi_{\beta+}$ is the wave function of the positron in the field of the electron to which it is bound and the field of the lattice, and r_e is now the classical electron radius.

This integral has been evaluated only for a very simplified lattice model (39). The basic assumption of the model is that positronium atoms move in a potential lattice of square potentials, each of height U_o with radius r_o and electron density ρ_o. Each potential represents an "excluded volume" V_o, centered in a cell of volume V_1 and radius r_1. Then for some r in the range $r_o \leq r \leq r_1$, $U_1 = 0$ and $\rho_1 = 0$. The difference $V_1 - V_o$ is the "free volume" of the cell and $V^* = \frac{V_1}{V_o}$ is defined as the reduced cell volume. Mutual positronium and lattice polarization is neglected, and the positronium atoms are assumed to be thermalized and are treated in the zero velocity approximation.

Then with

$$\Psi_{\beta+}(\vec{r}) = \Psi_{Ps}(\vec{r}_o)$$

where the subscript o refers to the positronium center of mass, equation (23) becomes

$$\gamma_p = \pi r_e^2 c \rho_o \int_{V_o} \Psi_{Ps}^* \Psi_{Ps} \, d^3\vec{r} \qquad (24)$$

Application of the Wigner-Seitz approximation to this integral gives

$$\gamma_p = \frac{\pi r_e^2 c \rho_o}{1 + F(U_o, r_o, r_1)} \qquad (25)$$

where F is a complicated function of the lattice parameters. This equation is not explicitly dependent on temperature since F is calculated in the zero velocity approximation

and the lattice is assumed to be adiabatically rigid.

The positronium mean lifetime τ_2 in terms of γ_p is

$$\tau_2^{-1} = \gamma_p + \gamma_3 \tag{26}$$

where γ_3 is the three quantum annihilation rate. But

$$\gamma_3 << \gamma_p$$

so

$$\tau_2 = \frac{1 + F(U_0, r_0, r_1)}{\pi r_e^2 c \rho_0} \quad . \tag{27}$$

Calling

$$\tau_0 = (\pi r_e^2 c \rho_0)^{-1}$$

obtain

$$\tau_2 = \tau_0 [1 + F(U_0, r_0, r_1)] \quad . \tag{28}$$

Since

$$P_0 r_0^2 = (4m/\hbar^2) U_0 r_0^2 \tag{29}$$

where $P_0 r_0^2$ is the scattering parameter, the expression for τ_2 may be rewritten as

$$\tau_2 = \tau_0 [1 + F(P_0 r_0^2, V^*)] \quad . \tag{30}$$

The complicated function F has been calculated for the cylindrical geometry of polymer lattices, and for spherical and planar geometry. Figure 14 is a plot of F versus reduced volume V^* for cylindrical geometry (39).

In order to use equation (30) for a particular substance, V_0 must be known or assumed; τ_0 can be calculated, but sometimes must be adjusted to give a good fit of τ_2 to experimental values. The reduced volume can be calculated from the equation of state of the substance, or obtained directly from specific volume data. For cylindrical geometry, at the condition of tightest packing,

$$V^*(T=0) = V_1(T=0)/V_0 = 2\sqrt{3}/\pi \tag{31}$$

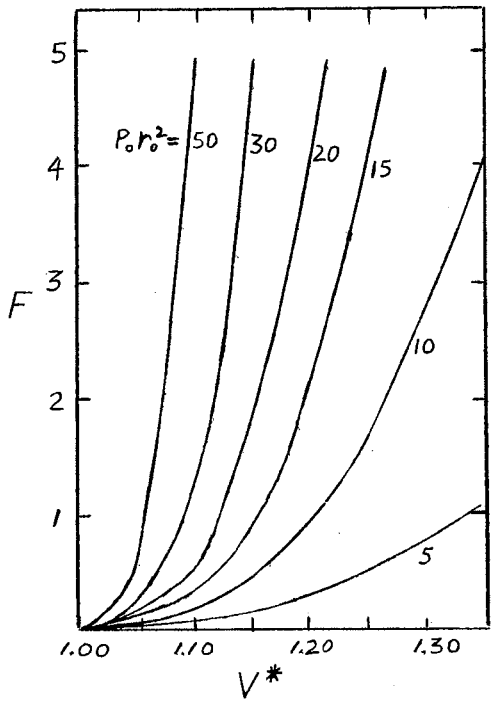

Figure 14. A Plot of the Function F Versus Reduced Volume for Cylindrical Geometry

where $V_1(T=0)$ is the specific volume at $T = 0^{\circ}K$.

Brandt, Berko, and Walker (39) have applied these calculations to Teflon, glycerol, and ice and water. The theoretical calculations agreed with the experimental results for Teflon and glycerol when some adjustments were made in τ_o and $P_o r_o^2$. The calculations broke down across the phase change from ice to water.

Similar calculations were carred out by the author for polystyrene, with the realization that this substance is amorphous to a high degree, and the agreement with experimental results is limited by that fact.

The polystyrene specific volume curve was extrapolated to absolute zero, and the specific volume at that temperature was substituted into equation (31) to get V_o. Then V^* at any

temperature was obtained by dividing the specific volume at that temperature by V_o. This method gave

$V^*(T = -196.5^oC) = 1.12$ $\quad$ $V^*(T = 23.7^oC) = 1.18$

$V^*(T = -78.5^oC) = 1.16$ $\quad$ $V^*(T = 44.6^oC) = 1.19$

$V^*(T = 122.0^oC) = 1.22$

The values of F were obtained directly from Figure 14.

Table II presents a list of calculated τ_2's for polystyrene, for two sets of values of τ_o and $P_o r_o^2$. The calculated value of τ_o is 0.52×10^{-9} second. The values of τ_2 for $\tau_o = 1.3 \times 10^{-9}$ second, $P_o r_o^2 = 10$ show the better agreement with experimental values. Figure 15 is a plot of τ_2 versus V^*, the reduced volume, showing the experimental points and the theoretically computed curve for $\tau_o = 1.3 \times 10^{-9}$ second and $P_o r_o^2 = 10$. The point marked T_g indicates the glass transition point. The agreement is fairly good up to T_g, but not so good for the high temperature point.

TABLE II

THEORETICAL CALCULATIONS FOR POLYSTYRENE

τ_o(sec.)	V^*	$P_o r_o^2$	F	τ_2 (sec.)
1.5×10^{-9}	1.12	7.5	0.20	1.80×10^{-9}
	1.16		0.35	2.02×10^{-9}
	1.18		0.35	2.02×10^{-9}
	1.19		0.60	2.40×10^{-9}
	1.22		0.90	2.85×10^{-9}
1.3×10^{-9}	1.12	10	0.30	1.69×10^{-9}
	1.16		0.60	2.08×10^{-9}
	1.18		0.80	2.34×10^{-9}
	1.19		0.90	2.47×10^{-9}
	1.22		1.25	2.93×10^{-9}

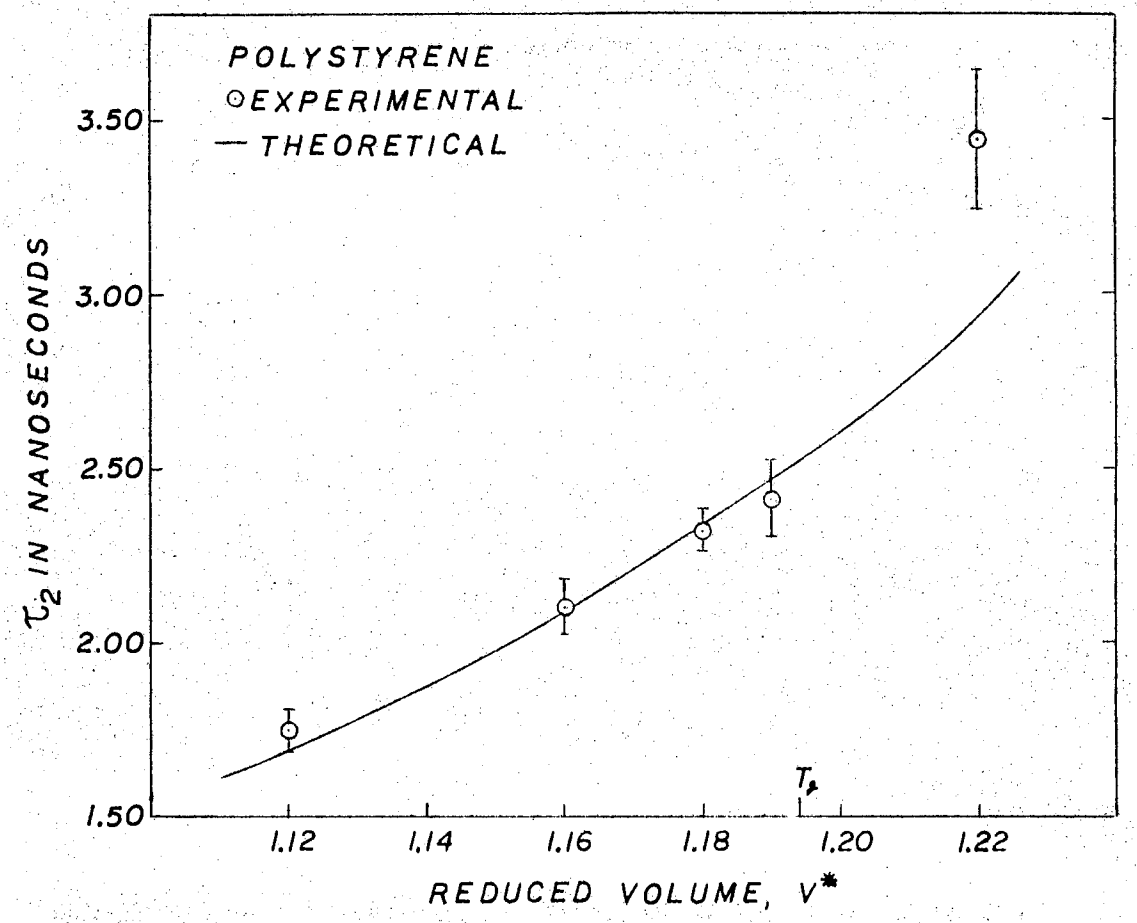

Figure 15. A Plot of Experimental and Theoretical Lifetimes Versus Reduced Volume
(Theoretical curve computed with $\tau_0 = 1.3 \times 10^{-9}$ second, $P_0 r_0^2 = 10$)

The upward adjustment of τ_0 in this process corresponds to decreasing the electron density, ρ_0. It is not known why this adjustment is necessary. A better fit of the experimental data could probably be made for polyethylene because of its more regular structure. Calculations were not made for Lucite and polyethylene due to lack of low temperature specific volume data, from which V^* is determined.

The above theory is a good first attempt at an explanation of the temperature variation of positronium lifetime. It probably works best on materials whose structures are almost completely ordered, but seems to run into trouble at phase changes. In terms of the theory, longer lifetimes at higher temperatures are due to larger free volumes which cause less overlap of positron and lattice wave functions. The opposite is true at lower temperatures.

Amorphous Sulfur

When sulfur is heated to 160°C, the ring molecules S_8 break up into long chain molecules, S_n. Upon cooling, this form of sulfur, called amorphous sulfur, is stable, and takes many days or even years to return to rhombic form (40). In structure, then, amorphous sulfur is similar to the polymers.

Colombino, et.al. (41) measured the angular correlation between gamma rays of positron annihilation in rhombic, monoclinic, and amorphous sulfur. Plots of count rate versus angle for materials in which positronium is being formed show a peaked, narrow distribution; other materials give a very broad angular distribution. In their experiment, the angular distributions of all three forms of sulfur were broad and very similar. On the basis of this evidence, one could conclude that a detectable amount of positronium is not formed in amorphous sulfur, so there should be no τ_2 component. However, if a large number of imperfections are

introduced in the making of the sample, then a small τ_2 component might be possible.

Stannic Oxide

The mean lifetime τ_1 was slightly longer in powdered stannic oxide than in the stannic oxide crystals. There was no evidence of a τ_2 component in either sample. The formation of positronium is improbable due to the attraction of positrons to the negative ions.

The difference in lifetimes may be due to one of two causes, or a combination of the two. The first is the difference in mass densities of the two samples. Since the powder was not tightly packed, a smaller mass density would be expected for it. In equation (22), assuming that ρ_0 is the density of outer shell electrons only (9), it can be replaced by

$$\rho_0 = LZd/A \tag{32}$$

where L is Loschmidt's number, d is the mass density of the material, Z is the number of outer shell electrons per atom, and A is the atomic mass. Then

$$\tau_1 \propto A/Zd \tag{33}$$

which shows that a smaller d gives a larger τ_1.

The second cause is the iron impurity atoms in the crystals. Providing these atoms are interstitial and not substitutional, two or three electrons are added to the lattice for each impurity atom. The electrons are essentially free and may be responsible for the shorter lifetime,

which is in the range of lifetimes found for metals. An easy verification of the effect of impurities on lifetimes would be a measurement of the lifetime in almost pure crystals.

Suggestions For Future Research

There is a great need for more lifetime data over the entire temperature range for the polymers. These measurements are to be made in the near future with essentially the same experimental design, but with certain electronic components replaced to give better resolution and less drift. Plans also call for the construction of a temperature regulation device for the copper rod so that sample temperatures can be controlled to within $\pm 1\ C^{o}$. This is essential for lifetime measurements near phase transitions.

Future high temperature lifetime measurements will need a cooling system for the photomultiplier tubes. Low temperature lifetime measurements between those already obtained can be made by putting one end of the copper rod in a dewar flask containing liquid nitrogen or dry ice, thereby cooling the sample by conduction. Further temperature adjustment can then be made by slight heating of one of the coils.

These measurements should also be extended to other materials of interest such as Teflon, graphite, and perhaps glasses. The interest in Teflon would be concentrated on the high temperatures, since much work has already been

done at low temperatures. This polymer has amazing thermal stability, and does not melt until heated to 327°C. Graphite has one of the longest τ_1 lifetimes at room temperature. Lifetime measurements in graphite at temperature extremes should be easily interpreted, since its structure is well known. Glasses are completely amorphous and may exhibit the τ_2 component.

Auxiliary experiments to determine the properties of all samples used should also be planned. The properties most vital to lifetime studies are density and percentage of crystallinity over a wide temperature range, as well as amount and type of impurities present. Some of these might be measured most easily by infra-red absorption or transmission.

Also of interest in positron annihilation studies are samples that have been exposed to radiation. Positronium might form in vacancies created by atoms that have been knocked out of their lattice sites. These measurements should be attempted in polymers and ionic crystals.

Angular correlation apparatus is presently being set up and should provide additional information concerning the electronic structure of materials.

BIBLIOGRAPHY

1. Anderson, C.D. "Energies of Cosmic Ray Particles." Physical Review, 41, 405-421 (1932).

2. De Benedetti, S. et. al., "On the Angular Distribution of Two-Photon Annihilation Radiation." Physical Review, 77, 205-212 (1950).

3. Mohorovičić, S. Astron. Nacht 253, 94 (1934).

4. Ruark, A.E. "Positronium." Physical Review, 68, 278 (1945).

5. Deutsch, M. "Evidence for the Formation of Positronium in Gases." Physical Review, 82, 455-456 (1951).

6. Deutsch, M. "Three Quantum Decay of Positronium." Physical Review, 83, 866 (1951).

7. Wheeler, J.A. "Polyelectrons." Annals of the New York Academy of Sciences, 48, 219-238 (1946).

8. Ferrell, R.A. "Theory of Positron Annihilation in Solids." Reviews of Modern Physics, 28, 308-337 (1956).

9. Wallace, P.R. "Positron Annihilation in Solids and Liquids." Solid State Physics, 10, 1-69 (1960).

10. De Zafra, R.L. and W.T. Joyner. "Temperature Effect on Positron Annihilation in Condensed Matter." Physical Review, 112, 19-29 (1958).

11. De Benedetti, S. and H.C. Corben. "Positronium." Annual Review of Nuclear Science, 4, 191-218 (1954).

12. Heitler, W. The Quantum Theory of Radiation, (Oxford, 1954) pp. 268-271.

13. Ore, A. and J.L. Powell. "Three Photon Annihilation of an Electron-Positron Pair." Physical Review, 75, 1696-1699 (1949).

14. Bell R.E. and R.L. Graham. "Time Distribution of Positron Annihilation in Liquids and Solids." Physical Review, 90, 644-654 (1953).

15. Landes, H.S. "Temperature Dependence of Positron Lifetime in Liquids and Solids." Ph.D. Thesis, University of Virginia (University Microfilms, Ann Arbor, Michigan).

16. Ferguson, A.T.G. and G.M. Lewis. "On the Annihilation of Positrons in Solids." Philosophical Magazine, 44, 1339-1347 (1953).

17. Landes, H.S., S. Berko, and A.J. Zuchelli. "Recent Experiments on Positron Lifetimes in Solids and Liquids." Bulletin of the American Physical Society Series II, 1, 68-69 (1956).

18. Lundholm, J.G., J.A. Bjorkland, and A.C. Menius. "Positron Lifetime in Plastics as a Function of Temperature." Bulletin of the American Physical Society Series II, 2, 173 (1957).

19. Graham, R.L. and A.T. Stewart. "Three Quantum Annihilation of Positrons in Solids." Canadian Journal of Physics, 32, 678-679 (1954).

20. Berko, S. and F.L. Hereford. "Experimental Studies of Positron Interactions in Solids and Liquids." Reviews of Modern Physics, 28, 299-307 (1956).

21. Shafroth, S.M. and J.A. Marcus. "Annihilation Radiation from Positrons Stopping in Superconducting Lead." Physical Review, 99, 664-665 (1955).

22. Graham, R.L., D.A.L. Paul, and D.G. Henshaw. "Annihilation Lifetimes of Positrons in Liquid Helium, Superconducting Lead, and Superconducting Vanadium." Bulletin of the American Physical Society Series II, 1, 68 (1956).

23. Paul, D.A.L. and R.L. Graham. "Annihilation of Positrons in Liquid Helium." Physical Review, 106, 16-18 (1957).

24. Wackerle, J. and R. Stump. "Annihilation of Positrons in Liquid Helium." Physical Review, 106, 18-20 (1957).

25. Stump, R."Influence of Pressure on Lifetime of Positrons in Amorphous Materials." Bulletin of the American Physical Society Series II, 2, 173 (1957).

26. Wallace, P.R. "Annihilation of Positrons in Condensed Materials." Physical Review, 100, 738-741 (1955).

27. Simms, P.C. "A Fast Coincidence System Based on a Transistorized Time to Amplitude Converter." To be published.

28. Beers, Y. Introduction to the Theory of Error (Addison - Wesley, 1957) pp. 26-35.

29. Bell, R.E. and M.H. Jørgensen. "Mean Lives of Positrons in Aluminum and the Alkali Metals." Canadian Journal of Physics, 38, 652-664 (1960).

30. Gerholm, T.R. "On the Annihilation of Positrons in Condensed Materials." Arkiv for Fysik, 10, 523-552 (1956).

31. Pigg, J.L. "Variation of Positronium Lifetime With Temperature -- Electronic System of Measurement." Unpublished M.S. Thesis, Oklahoma State University, 1962.

32. Eagleton, R.D. "Temperature Dependence of Positron Annihilation." Unpublished M.S. Thesis, Oklahoma State University, 1961.

33. Billmeyer, F.W. Jr. Textbook of Polymer Chemistry. Interscience Publishers, Inc. New York, 1957.

34. Fleck, H.R. Plastics - Scientific and Technological. pp. 168-172, Chemical Publishing Co, Inc., Brooklyn, New York, 1949.

35. Fox, T.G. and P.J. Flory. "Second-Order Transition Temperatures and Related Properties of Polystyrene." Journal of Applied Physics, 21, 581-591 (1950).

36. Kakudo, M. and R. Ullman. "Polyethylene Crystallinity from X-Rav Studies." Journal of Polymer Science, 45, 91-104 (1960).

37. Ohlberg, S.M. and S.S. Fenstermaker. "The Determination of the Glass Transition Temperature of Polyethylene by X-Ray Diffraction." Journal of Polymer Science, 32, 514-516 (1958).

38. Landes, H.S., S. Berko, and A.J. Zuchelli. "Effect of Melting on Positron Lifetime." Physical Review, 103, 828-829 (1956).

39. Brandt, W., S. Berko, and W. Walker. "Positronium Decay in Molecular Substances." Physical Review, 120, 1289-1295 (1960).

40. Schenk, J. "Some Properties of Liquid Sulfur and the Occurrence of Long Chain Molecules." Physica, 23, 325-337 (1957).

41. Colombino, P., et.al. "Angular Correlation of Annihilation Radiation in Sulfur and Its Compounds." Physical Review, 119, 1665-1666 (1960).

42. Bay, Z., V.P. Henri, and H. Kanner. "Statistical Theory of Delayed-Coincidence Experiments." Physical Review, 100, 1197-1208 (1955).

APPENDIX A

Temperature Regulation Data

The following table represents temperature regulation data for the heating rod described in Chapter II. The previously mentioned thermocouple and potentiometer method was used to measure the temperature of a plastic sample inserted in the rod. Three different voltages were tried.

Voltage	Temperature	Time in Hrs. and Min.
20.0 volts	61.6°C	0:00
	63.5°C	0:13
	63.5°C	0:20
	62.2°C	0:28
	60.2°C	0:40
	60.4°C	0:50
	61.6°C	0:59
	62.0°C	1:02
	62.0°C	1:03
	64.0°C	1:07
	63.0°C	1:10
	63.0°C	1:15

The midpoint in this range of temperatures is 62.1°C. The temperature for this data run may be reported 62.1 ± 1.9°C.

Voltage	Temperature	Time in Hrs. and Min.
30.5 volts	98.8°C	0:00
	97.8°C	0:07
	97.0°C	0:12
	99.2°C	0:19
	99.3°C	0:25
	99.3°C	0:30

Voltage	Temperature	Time in Hrs. and Min.
30.5 volts (continued)	100.2°C	0:36
	100.2°C	0:51
	99.8°C	0:55

For this run, 98.6 ± 1.6°C is the temperature.

Voltage	Temperature	Time in Hrs. and Min.
44.5	188.5°C	0:00
	188.8°C	0:05
	189.0°C	0:07
	189.2°C	0:08
	189.2°C	0:10
	189.4°C	0:12
	189.6°C	0:17
	189.8°C	0:20
	190.0°C	0:24
	190.0°C	0:27
	190.2°C	0:32
	190.3°C	0:35

The temperature on this run had not yet reached its maximum and turned back, but had only increased 1.8°C over thirty-five minutes.

APPENDIX B

Sample Data Sheet

The following is a sample data sheet as typed out by the IBM electronic typewriter. It gives the number of coincidences in each channel. The sample is that of polystyrene at room temperature.

000011	000131	000444	001610	001597	001278	001101	000977
000885	000834	000750	000740	000721	000748	000775	000792
000967	001183	001463	001855	002249	002843	003234	003679
004208	004858	005017	005488	005565	005730	005771	005624
005472	005408	004885	004521	004224	003890	003604	003269
002852	002594	002347	002035	001909	001707	001586	001452
001288	001192	001111	001034	000977	000799	000828	000707
000712	000667	000627	000530	000521	000531	000438	000493
000451	000420	000412	000371	000373	000355	000321	000252
000297	000260	000268	000251	000267	000253	000222	000210
000207	000198	000201	000191	000188	000183	000157	000174
000146	000166	000168	000162	000137	000141	000154	000127
000139	000145	000132	000141	000128	000128	000133	000112
000120	000094	000106	000093	000081	000084	000096	000073
000092	000072	000072	000077	000064	000075	000060	000063
000042	000056	000051	000049	000049	000048	000044	000046
000059	000032	000046	000034	000050	000030	000037	000045
000025	000025	000023	000038	000032	000036	000038	000032
000032	000023	000039	000045	000034	000034	000028	000035
000016	000005	000000	000000	000000	000000	000000	000000
000000	000000	000000	000000	000000	000000	000000	000000

APPENDIX C

The Least Squares Fit and the Folding Process

The fit of a straight line $Y = \lambda C + b$ to the points Y_i (natural logarithm of the number of counts), C_i (channel number) by the following weighted least squares method (42,15) gives the "most probable" equation for Y. With N_i, the number of counts, as weighting factors, the slope and intercept are given by

$$\lambda = \frac{\sum_i N_i (C_i - \bar{C})(Y_i - \bar{Y})}{\sum_i N_i (C_i - \bar{C})^2} \qquad \text{(a)}$$

$$b = \frac{\bar{Y} \sum_i N_i C_i^2 - \bar{C} \sum_i N_i C_i Y_i}{\sum_i N_i (C_i - \bar{C})^2} \qquad \text{(b)}$$

where

$$\left.\begin{aligned} \bar{C} &= \frac{\sum_i N_i C_i}{\sum_i N_i} \\ \bar{Y} &= \frac{\sum_i N_i Y_i}{\sum_i N_i} \end{aligned}\right\} \qquad \text{(c)}$$

and

$$Y_i = \ln_e N_i \ . \qquad \text{(d)}$$

Then the mean lifetime is

$$\tau_2 = \frac{1}{\lambda}(\text{channels}) \times k\left(\frac{10^{-9}\ \text{sec.}}{\text{channels}}\right), \qquad \text{(e)}$$

k being the instrument calibration constant.

The variance in $\frac{1}{\lambda}$ is

$$\sigma_r = \frac{(1/\lambda)^4}{\sum_i N_i (c_i - \bar{c})^2} \qquad (f)$$

The square root of the variance is the standard deviation of the reciprocal of the slope, and when converted to nanoseconds by multiplication by k, gives the uncertainty in τ_2.

As mentioned in Chapter III, an experimental curve is a composite of the apparatus resolution curve, or "prompt" curve, and the coincidence curve due to the annihilation of positrons in the sample. Providing the drop off rate due to the coincidence apparatus is less than the mean lifetime of positrons in aluminum, an aluminum time distribution curve corrected for positron lifetime in aluminum, can serve as a prompt curve.

Defining $F(x)$ as the coincidence curve, $P(x)$ the "prompt" curve, X the time difference in pulses accepted as a coincidence at the time to amplitude converter, and $f(t)$ as the probability of a positron annihilating between times t and $t + dt$, the equation for the coincidence curve is (42,15)

$$F(x) = \int_{-\infty}^{+\infty} f(t)\, P(x - t)\, dt \qquad (g)$$

The function $f(t)$ becomes

$$f(t) = \lambda e^{-\lambda t} \qquad t > 0$$
$$f(t) = 0 \qquad t < 0 \qquad (h)$$

because positrons decay exponentially with time. Here λ is the decay constant in reciprocal seconds. Then

$$F(x) = \lambda \int_0^{\infty} e^{-\lambda t}\, P(x - t)\, dt \qquad (i)$$

If the "prompt" curve is symmetrical, $P(x)$ can be replaced by a Gaussian distribution. When it is assymetric, as in this case, the integral is replaced by

$$F(x) = \sum_{x=0}^{n} P(x-x)\,\lambda\, e^{-\lambda x} \qquad (j)$$

The coincidence curve is folded out of the composite curve by a numerical integration. A plot of the values of $F(x)$ then yields the coincidence curve, or τ_2 component, as it has been called.

Differentiation of (i) with respect to X gives

$$\frac{dF(x)}{dx} = \lambda\left[P(x) - F(x)\right]$$

$$\frac{d \ln F(x)}{dx} = -\lambda\left[1 - \frac{P(x)}{F(x)}\right]$$

$$\cong -\lambda \qquad (k)$$

when $F(x) >> P(x)$. This justifies equation (e). The slope of the $F(x)$ curve on semi-logarithmic paper leads to the reciprocal of the mean lifetime.

The centroid of $F(x)$ is shifted positively an amount $\frac{1}{\lambda}$ from the centroid of $P(x)$ along the time or channel number axis. The intensity of the τ_2 component is the ratio of the area of $F(x)$ to the area of the composite curve (15).

The actual process of determining the intensity, I_2, and τ_2 by the centroid shift will now be outlined. The aluminum and composite experimental curves are plotted on the same sheet of semi-logarithmic graph paper. The centroid of the $P(x)$ curve is then obtained by dividing the net

moments about an arbitrary point under the curve by the area under the curve. The area may be found by Simpson's rule. Now this curve is corrected for the lifetime of positrons in aluminum by shifting it to the left along the time or channel number axis an amount equal to the lifetime in aluminum. (in this experiment, 1.9×10^{-10} second). Then the centroid of the $P(x)$ curve lies on the true zero of time. This shifting of the $P(x)$ curve actually determines the true zero. The ordinates of $P(x)$ are read off the curve at regular intervals of X , and are placed in the indicated column of Table III. How this table is used in the folding process will be explained later. Next the straight line portion of the $F(x)$ curve is drawn back to the true zero point. The ordinates of this straight line at intervals of X equal to that used for $P(x)$ are then recorded in the indicated row of Table III, after being multiplied by a constant appropriate for the use of Simpson's rule. The folding process of equation (j) then proceeds by multiplying every value of $P(x)$ by every value of $A e^{-\lambda t}$, and placing the product of each multiplication in the proper square of Table III. Summing these products diagonally from upper left to lower right gives the values of $F(x)$, times some constant. The values of $F(x)$ must be plotted on another sheet of semi-logarithmic paper, and this curve is matched to the composite curve so that the straight line portions coincide. Then the $F(x)$ curve may be traced on to the original graph paper. Subtraction of this component from

the composite curve leaves the τ_1 component. Figure 16 shows a composite curve and the τ_1 and τ_2 components. The displacements of the centroids of these components from true zero determine the mean lifetime values.

An alternate method of obtaining the intensity I_2 is to plot the composite curve and $F(x)$ curve on linear graph paper, and use a planimeter to determine their areas. The ratio of the area of $F(x)$ to the area of the composite curve is I_2.

		t →	0	5	10	15	20	25	30	35	40	45	50	55	60	65	70	75	80	
X	P(x)	$Ae^{-\lambda t}$ →	917	3068	1269	2121	876	1461	603	1007	416	694	286	474	196	327	137	227	93	
+25	11		10.1*	33.7	13.9	23.3	9.6	16.1												
+20	66		60.5	202.5	83.8	140.0	57.8	96.4	39.8											
+15	280		256.8	859.0	355.3	593.9	245.3	409.1	168.8	282.0										
+10	870		797.8	2669.2	1104.0	1845.3	762.1	1271.1	524.6	876.1	361.9									
+5	1850		1696.4	5675.8	2347.6	3923.8	1620.6	2702.8	1115.6	1862.9	769.6	1283.9								
0	2300		2109.1	7056.4	2918.7	4878.3	2014.8	3360.3	1386.9	2316.1	956.8	1596.2	657.8							
-5	1600		1467.2	4908.8	2030.4	3393.6	1401.6	2337.6	964.8	1611.2	665.6	1110.4	457.6	758.4						
-10	800		733.6	2454.4	1015.2	1696.8	700.8	1168.8	482.1	805.6	332.8	555.2	228.8	379.2	156.8					
-15	330		302.6	1012.4	418.8	699.9	289.1	482.1	199.0	332.3	137.3	229.0	94.4	156.4	64.7	107.9				
-20	120		110.0	368.2	152.3	254.5	105.1	175.3	72.4	120.8	49.9	83.3	34.3	56.9	23.5	39.2	16.4			
-25	37		33.9	113.5	47.0	78.5	32.4	54.1	22.3	37.3	15.4	25.7	10.6	17.5	7.3	12.1	5.1	8.4		
-30	11		10.1	33.7	13.9	23.3	9.6	16.1	6.6	11.1	4.6	7.6	3.1	5.2	2.2	3.6	1.5	2.5	1.0	

F(x) → 10.1 | 67.6 | 237.4 | 741.1 | 1986.4 | 4643.4 | 8898.8 | 12977.8 | 14082.1 | 13,065.1 | 11,193.1 | 7400.9 | 7790.2 | 6485.0 | 5367.2 | 4465.0

X → -30 -20 -10 0 +10 +20 +30 +40

* ALL PRODUCTS AND SUMS ARE X10^3

TABLE III

SAMPLE FOLDING PROCESS TABLE

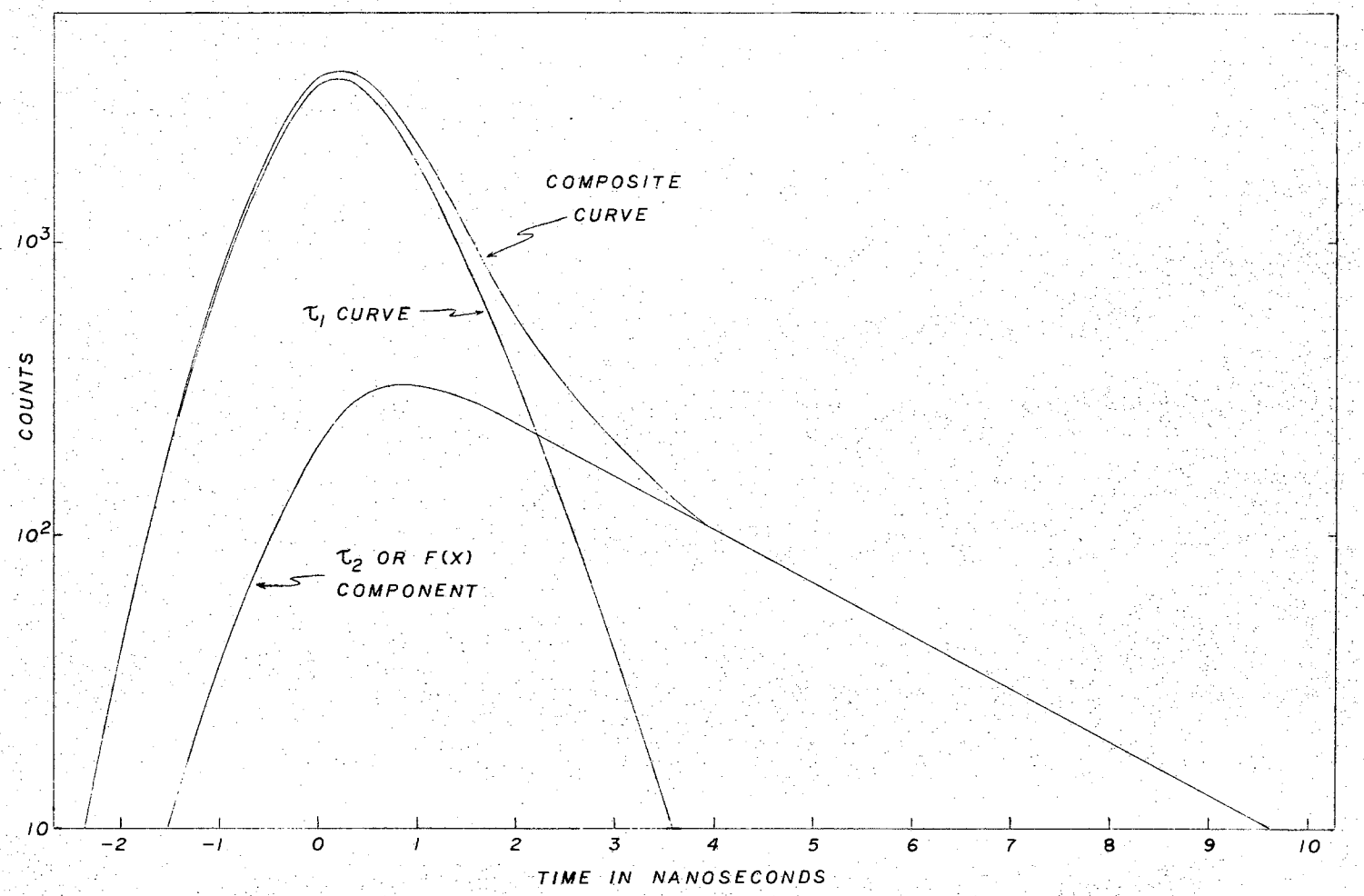

Figure 16. Illustration of an Experimental Composite Curve and the τ_1 and τ_2 Components

VITA

Gerald Dean Loper, Jr.

Candidate for the Degree of

Master of Science

Thesis: THE VARIATION OF THE ANOMALOUS POSITRON LIFETIME WITH TEMPERATURE IN SOLIDS

Major Field: Physics

Biographical:

Personal Data: Born May 4, 1937, in Brooklyn, New York, the son of Johanna L. and Gerald D. Loper.

Education: Attended grade school in Brooklyn and Wichita, Kansas. Graduated from Wichita High School East in 1955. Conducted undergraduate studies at the University of Arizona and the University of Wichita; received the Bachelor of Arts degree from the latter institution with a major in Physics in May, 1959. Completed requirements for the Master of Science degree from the Oklahoma State University, with a major in Physics, in May, 1962.